Development of Magnetic Nanomaterials and Devices for Biological Applications

DARPA Grant No. HR0011-04-C-0068

FINAL TECHNICAL REPORT

October 30, 2007

Submitted to:

Defense Advanced Research Projects Agency
3701 North Fairfax Drive
Arlington, VA 22203-1714

by

Charles J. O'Connor
Advanced Materials Research Institute, College of Sciences
University of New Orleans, New Orleans, LA 70148
Phone: (504) 280-6840, Fax: (504) 280-3185
e-mail address: coconnor@uno.edu

Co-PIs: Josef Hormes (LSU-CAMD)
Nicolas Bazan (LSU-NCE)

This Material is based upon work supported by the
Defense Advanced Research Projects Agency
Defense Sciences Office (DSO)
Effort/Program Title
ARPA Order No. S327/00
Issued by DARPA/CMO under Contract No. HR0011-04-C-0068

Development of Magnetic Nanomaterials and Devices for Biological Applications

Charles J. O'Connor
Advanced Materials Research Institute, College of Sciences
University of New Orleans, New Orleans, LA 70148
Phone: (504) 280-6840, Fax: (504) 280-3185
e-mail address: coconnor@uno.edu
Co-PI's: Josef Hormes (LSU-CAMD)
Nicolas Bazan (LSU-NCE)

Nanoparticles have been used in the form of adjuvants and drug delivery systems [1] and an extensive review of nanoparticles in medicine and pharmacy has been reported [2]. Nanoparticles are of great interest because they exhibit interesting chemical, thermal, optical, electrical and/or magnetic properties, and they find a variety of potential applications in diverse fields of research. Nanoparticles have found considerable utility as controlled drug delivery systems [3]. When suitably encapsulated, a drug or specific specie of interest can be directed to the appropriate site. Because of their small size nanoparticles can easily be injected into the circulatory system.

Magnetic nanoparticles have been used in biomedical research on cell separation, for magnetically targeted drug delivery, for protein and DNA purification, and for contrast enhancement in magnetic resonance imaging (MRI) [3-6]. Recently researchers have investigated the use of magnetic nanoparticles for medical treatment and diagnosis [7-9]. However, currently used magnetic nanoparticles are unstable under normal storage conditions due to aggregation and oxidation. Advances need to be made in order to form more stable formulations. Commercially available magnetic nanoparticles are suitable for cell separation where a large number of particles are used to separate a single cell from a sample. The magnetic moment of these particles is not high enough to enable the separation of single antigen molecules using a single particle. Bio-compatible, high sensitive magnetic sensors capable of detecting single magnetic nanoparticles are needed. In this project we explored the development of novel, bio-compatible ferrofluids of functionalized magnetic nanoparticles suitable for bioconjugation of antibodies or other active biomolecules. The fabrication and functionalization of the particles was carried out at AMRI at UNO.

Researchers in CAMD, conducted studies on the characterization of the electronic and eometric structure of magnetic functionalized nanoparticles using EXAFS and XANES techniques.

The LSU Neuroscience Center of Excellence (LSUNCE) in New Orleans. LSUNCE researchers developed molecular-recognition processes and identified bioreceptor-recognition elements needed to develop nanobiotechnologic approaches to (a) decrease the short-term consequences of mild traumatic head injury; (b) prevent or slow down laser-induced retinal injury; and c) to effectively manage pain in military personnel. This project was is a continuation of the work started in the project "Bio-Magnetics Interfacing Concepts: A Microfluidic System using Magnetic Nanoparticles for Quantitative Detection of Biological Species," DARPA Grant No. MDA972-03-C-0100.

A detailed description of the biomagnetic projects that were conducted by researchers in AMRI, CAMD and LSUHSC are described in the following sections. Collaborative activities between the consortium researchers are noted and emphasized throughout the text in bold font.

References

[1] A. Zimmer, Methods: A Companion to Methods in Enzymology, 18 (1999) 286-295.
[2] J. Kreuter, Marcel Dekker, New York (1994).
[3] J. Hanes, J.L. Cleland, and R. Langer, 28 (1997) 97-119.
[4] R. Weissleder, P.F. Hahn, D.D. Stark, G. Elizondo, S. Saini, L.E. Todd, J. Wittenberg, and J.F. Ferrucci, Radiology, 169 (1988) 399-403.
[5] Weissleder, R., et al., Radiology, 175 (1990) 489-93.
[6] S. Østergaard, G. Blankenstein, H. Dirac, and O. Leistiko, J. Magnetism and Magnet. Mat., 194 (1999) 156-162.
[7] C. Alexiou, W. Arnold, R.J. Klein, F.G. Parak, P. Hulin, C. Bergemann, W. Erhard, S. Wagenpfeil, and A.S. Lübbe, Cancer Research 60 (2000) 6641-6648.
[8] C.W. Jung, J.M.. Rogers, and E.V. Groman, J. Magnetism and Magnet. Mat., 194 (1999) 210-216.
[9] O.A. Kuznetsov, N.A. Brusentsov, A.A. Kuznetsov, N.Y. Yurchenko, N.E. Osipov, F.S. Bayburtskiy, J. Magnetism and Magnet. Mat., 194 (1999) 83-89.

PART 1 – AMRI Report
Development of Magnetic Nanomaterials and Devices for Biological Applications
DARPA Grant No. HR0011-04-C-0068

Advanced Materials Research Institute
College of Sciences, University of New Orleans
New Orleans, LA 70148

The AMRI research team defined two task objectives for the project:

Task 1 – Development of new and advanced synthetic methodology for the preparation of magnetic nanocomposite particles including magnetite-gold and magnetite-semiconductor nanocomposites. This task was performed by the Charles J. O'Connor, Zeev Rosenzweig, and Matthew Tarr groups.

Task 2 – Application of magnetic nanocomposite particles in drug delivery. This task was performed by the Zeev Rosenzweig, Nitsa Rosenzweig, and the Weilie Zhou groups.

Both task objectives are extremely important as they present clear potential for significant technical impact on the field of magnetic nanoparticle synthesis. The specific projects were chosen due to their potential to transform the field and to result in a wide range of biological applications. A description of the research activities and major findings of the groups is given below:

A) Synthesis Projects

Project 1 - Synthesis of gold-containing magnetic particles and composites - O'Connor and coworkers developed new synthetic strategies to form gold-coated magnetic nanoparticles of corrosion-resistant alloys and gold/magnetite nanocomposites by functionalizing the gold coatings/particles through Au-S bonds. Previously reported gold-coated Fe20Ni80 nanoparticles have been first subjected to a series of thermal annealing processes (200-500C) in order to determine the effects of annealing on the size and magnetic properties of the alloy. As the annealing temperature was increased from room temperature to 500C, the blocking temperatures were found to increase from 30K in the as-prepared material to a maximum of about 140K in the sample annealed at 400C. Above 400C, the particles became ferromagnetic due to an increase in the effective particle size of the magnetic cores to above 10 nm, which is the critical diameter for the observation of superparamagnetic behavior in these materials. Additionally, Dr.

O'Connor's group developed a method for preparing magnetite(Fe3O4)/Au nanocomposite materials by combining surface-treated magnetite nanoparticles with very small (< 5 nm) Au nanoparticles in colloidal form. This approach was undertaken due to the extreme difficulty in preparing gold-coated magnetite nanoparticles. The materials they have prepared are best described as nanocomposites consisting of ~3 nm Au particles decorating the surfaces of 10-15 nm Fe3O4 particles. The magnetic properties of the magnetite particles do not appear to be adversely affected by the presence of the Au. Furthermore, the Au nanoparticles appear to be tightly bound to the Fe3O4 surfaces, as they could not be removed by sonication/washing.

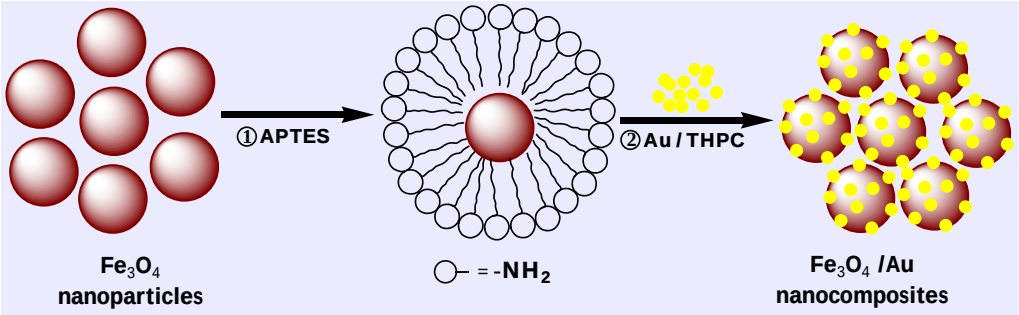

Figure 1 – Illustration of the synthesis of magnetite-gold nanocomposites.

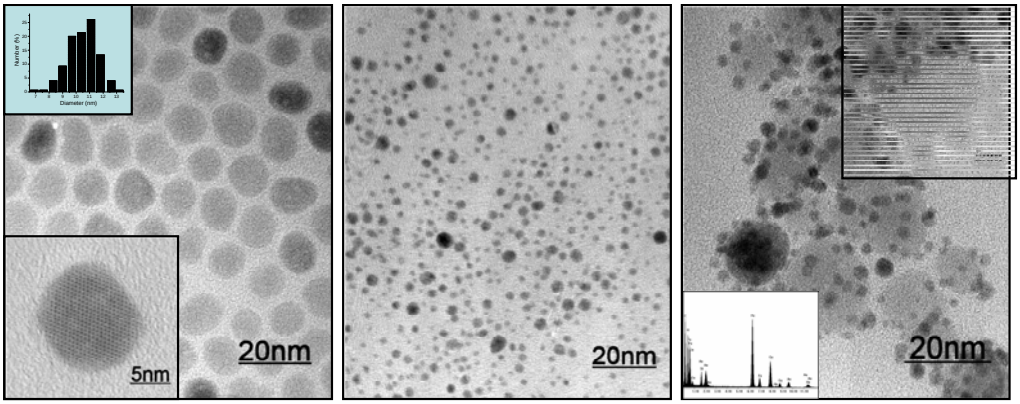

Figure 2 – High resolution TEM images of (left) Fe3O4 magnetite nanoparticles, (upper insert – size distribution, lower insert – a magnified image of a single magnetite nanoparticle), (center) gold nanoparticles, (right) Magnetite-gold nanocomposites (lower insert – EDS analysis showing iron and gold in the nanocomposites, upper insert – a magnified image of a single gold-magnetite nanocomposite particle showing gold nanocrystals decorating a magnetite nanoparticle.)

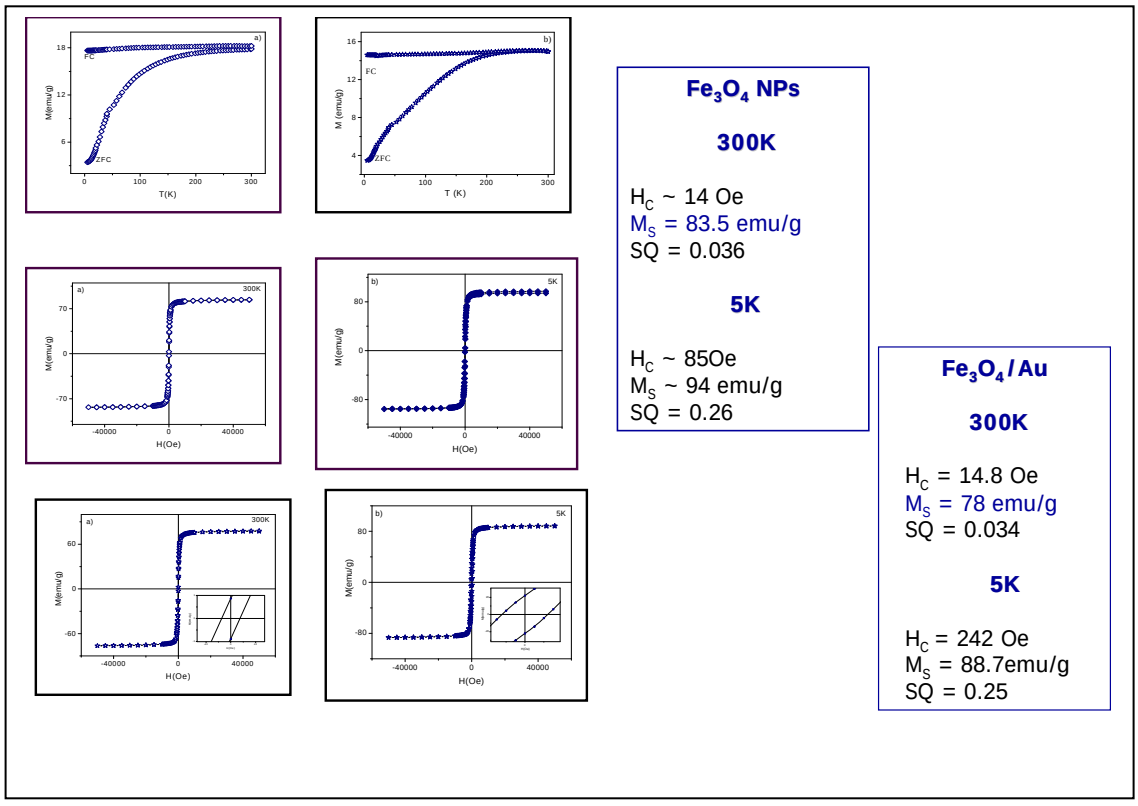

Figure 3 – Magnetic properties of magnetite nanoparticles (left) and gold-magnetite composites (right). The measurements reveal minimal changes in Hc at 300K but a 3-fold increase in Hc at 5K. The blocking temperature and Ms do not change significantly due to immobilization of gold nanocrystals on the surface of the magnetite particles.

Project 2 - Sonochemical Synthesis of Functionalizable Magnetic Nanoparticles – The Tarr group has focused on the synthesis of gold-magnetite and gold-magnetite-TiO2 nanocomposites using sonochemical techniques. While very easy to perform and rapid (synthesis is completed in 2 minutes), this method does not allow sufficient control of size and properties as the directed synthetic methods described above.

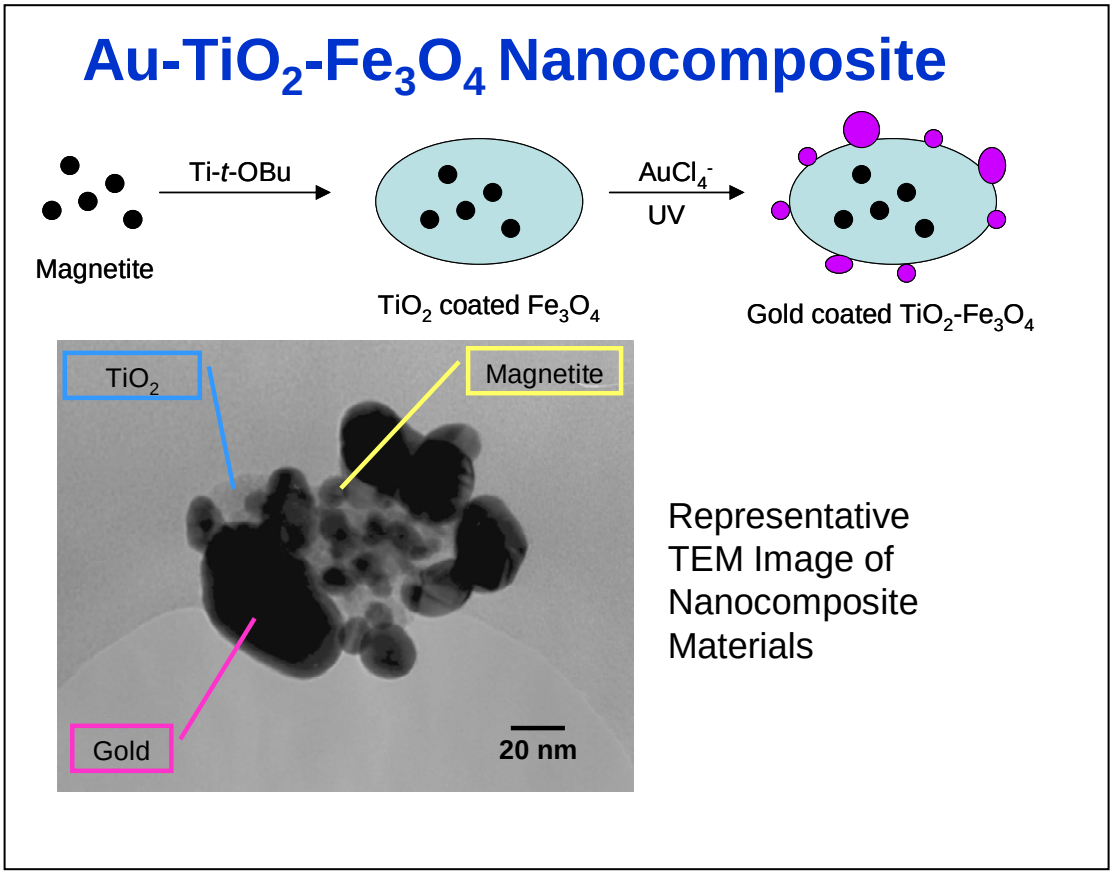

Figure 4 – Illustration of the synthesis and a representative TEM image of gold-magnetite-TiO2 nanocomposite particle. The magnetic and optical properties of the composite were not significantly altered due to the nanoparticle assemply.

2) Synthesis of polystyrene nanocomposite particles containing magnetite and cdSe/ZnS semiconductor nanocrystals – Rosenzweig, Z. and coworkers formed polystyrene nanocomposites containing magnetite and semiconductor nanocrystals of CdSe/Zns and characterized their structural, magnetic and luminescent properties. Polystyrene particles were prepared in the presence of magnetite and semiconductor nanocrystals to form the nanocomposite particles, which averaged 200 nm in diameter. Magnetic relaxation measurements were indicative of the aggregation state of the composites. SQUID magnetometry measurements of the composites showed variation in the blocking temperature between freely diffusing magnetite nanoparticles and the silica/magnetic composites. While the magnetic hysteresis curve was typical of superparamegnetic particles the blocking temperature was higher for the silica/magnetic nanocomposite materials, indicating a ferromagnetic like behavior of large

nanocomposites at the order of 200 nm in size. The luminescent properties of the polystyrene nanocomposites were characterized as well. The luminescence properties of the encapsulated semiconductor nanoparticles (quantum dots) remained largely unchanged with minimal increase in peak width.

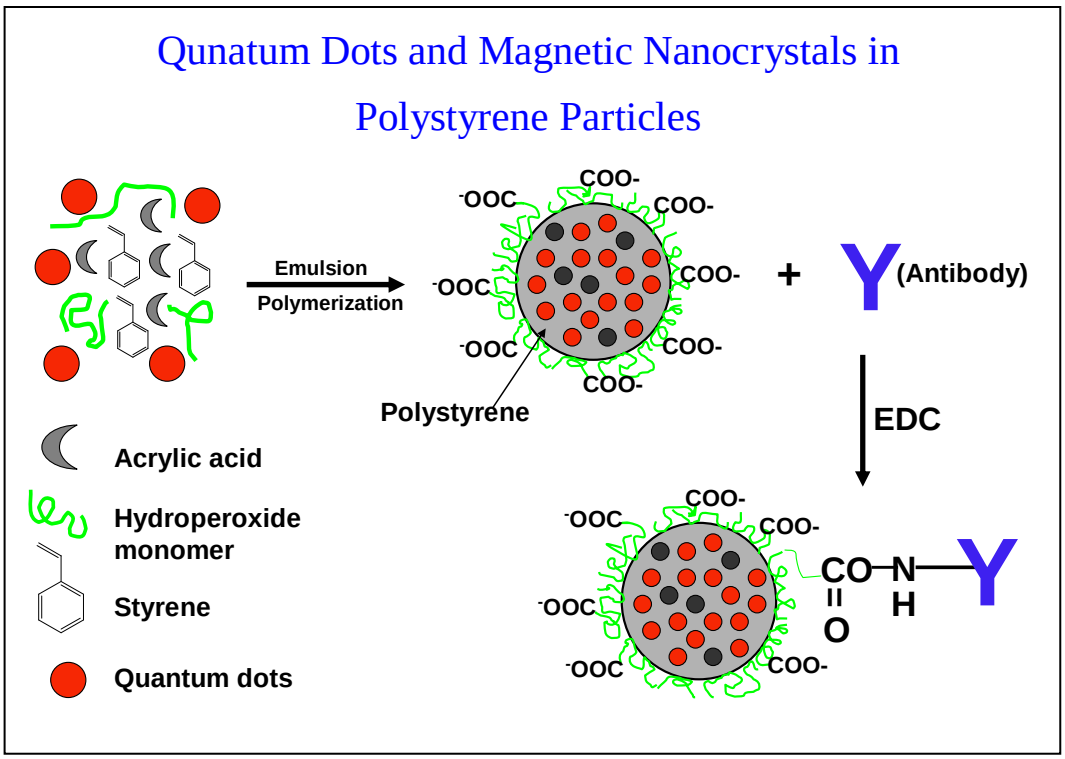

Figure 5 – Illustration of the preparation of polystyrene nanocomposite particles containing magnetite and CdSe/ZnS nanocrystals with subsequent surface modification with antibody molecules to enable bioassays applications.

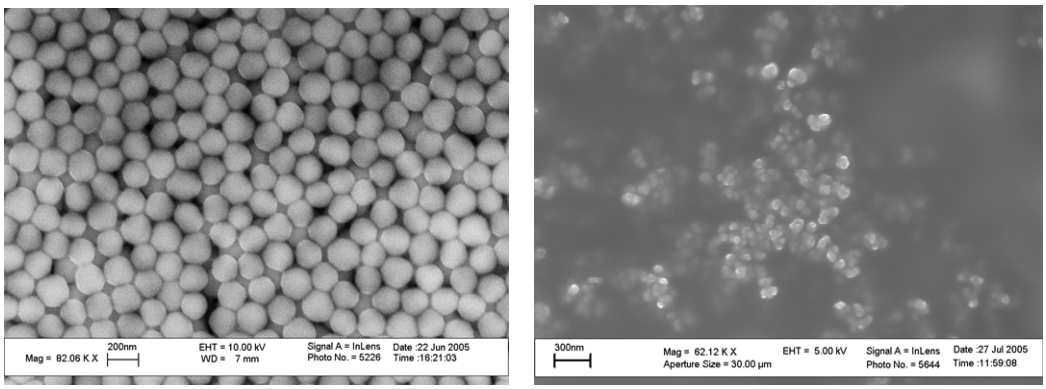

Figure 6 – TEM images of 200 nm polystyrene particles (left) and polystyrene particles containing magnetite and CdSe/ZnS luminescent nanocrystals

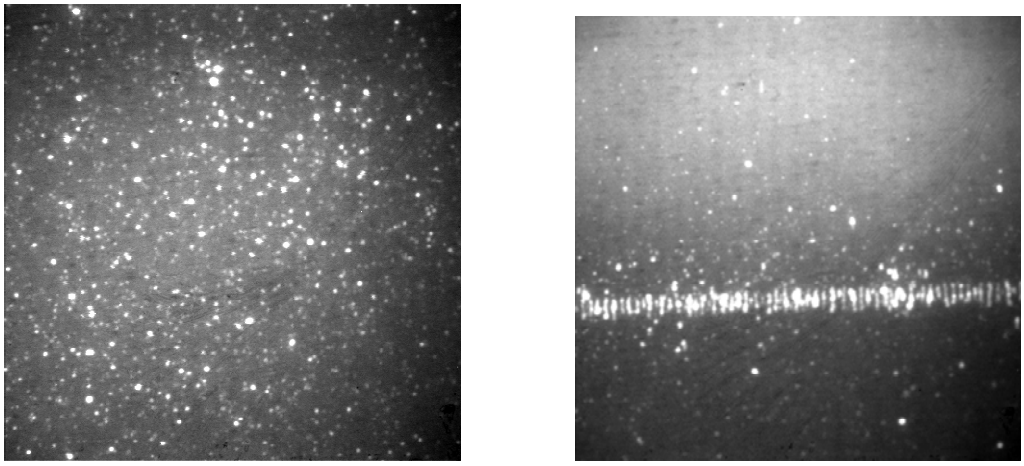

Figure 7 – Fluorescence images of polystyrene composite nanoparticles containing magnetite and CdSe/ZnS nanocrystals in the absence (left) and presence (right) of magnetic filed. The images show that the particles are both luminescent and magnetic.

B) Application Projects

1) Synthesis of biodegradable polymer films and particles for drug delivery applications –Rosenzweig, N. and coworkers focus their research on the synthesis of biodegradable collagen polymer films and particles for controlled drug release applications. During the reporting period they collagen gels 2 with varying cross linking level. They showed that the release rate of a model drug from the gel could be attenuated by increasing the cross linking level in collagen gels, which results in increasing resistance to enzymatic degradation by collagenase. The group also synthesized collagen gels that contain varying density of magnetite nanopareticles. Their studies showed that it is possible to mechanically perturb the gels by applying alternating magnetic fields at the order of 200 Gauss on the magnetic nanoparticles-containing gels. The rapid movement of the particles in the gels increase the gel porosity, which results in faster degradation of the gel by collagenase and therefore in faster drug release.

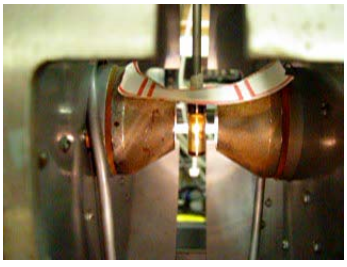

Figure 8 – Electromagnetic field apparatus used to apply an alternation 200 Gauss field on collagen films containing Fe_3O_4 magnetic nanoparticles.

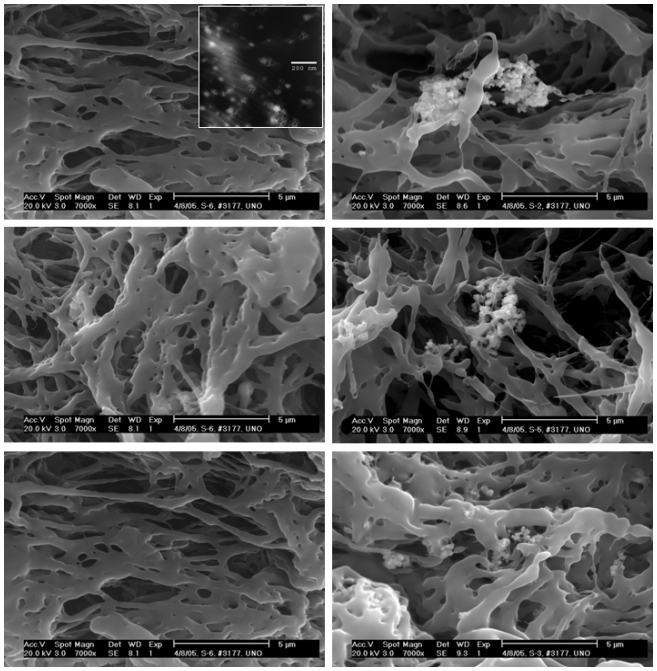

Figure 9 – SEM images of collagen gels containing Fe3O4 magnetic nanoparticles (left) and microparticles (right). The upper panels show the gel prior to application of an alternating magnetic field. The middle panels show the extent of structural damage to the gels following application of an alternating magnetic field for 5 minutes. It is clear that magnetic microparticles cause larger structural damage to the gel. The lower panels show the structure of the gels following 6 hours rest. The gel containing magnetic nanoparticles show full recovery while the gel containing microparticles is still damaged.

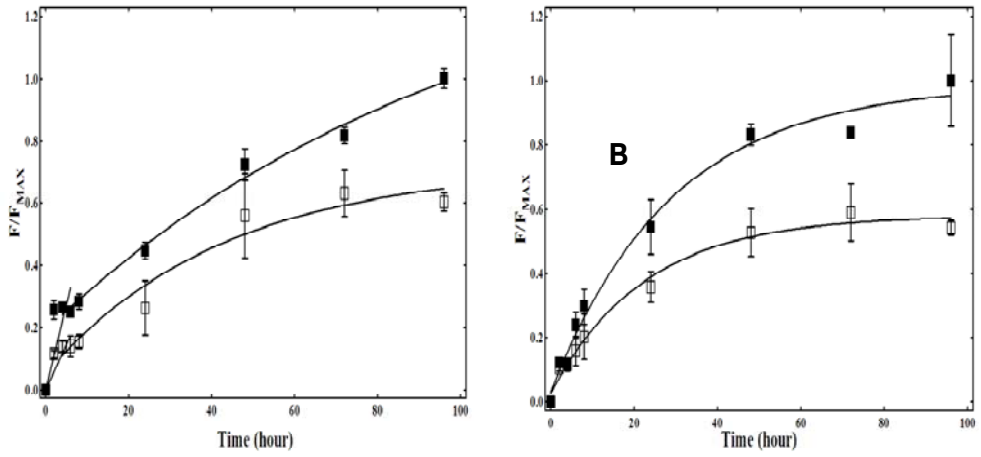

Figure 10 - Collagen gels containing (A) magnetic nanoparticles and (B) magnetic microparticles in the absence (□) and presence (■) of OMF. The Dex-R molecular weight was 70,000 g/mol. The release rate of Dex-R increased in both cases. An initial release burst was observed when nanoparticles rather than microparticles were embedded in the gel. A semi-emprical model was developed to describe the release rate for both systems.

2) Synthesis and applications of magnetic hollow silica nanocomposites – The Zhou group has focused on the synthesis of magnetic hollow silica nanocomposites (MHSNC), including nanospheres and nanotubes, for drug delivery applications. The group successfully developed a one-pot synthetic method to fabricate these promising structures.

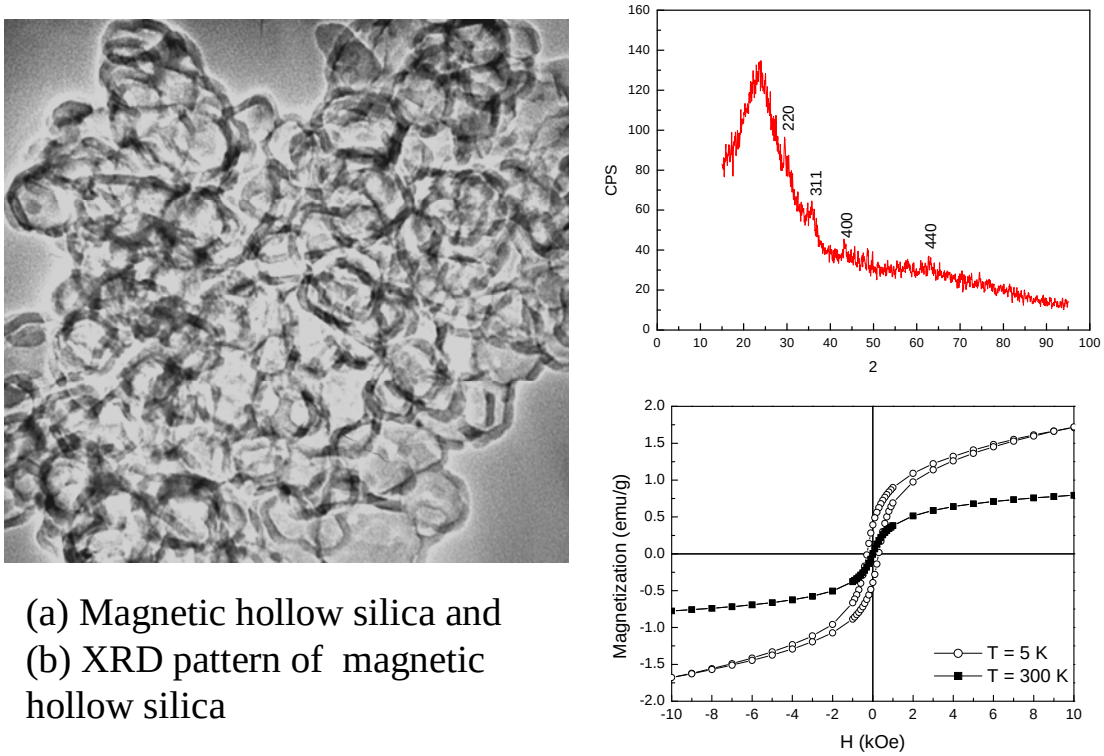

(a) Magnetic hollow silica and (b) XRD pattern of magnetic hollow silica

Figure 11 – A TEM image (left) and XRD and SQUID data (right) showing the formation of magnetic hollow silica round shape tubes. These structures are currently tested as drug delivery carriers.

List of Publications

1) AMRI Publications 2004-07 – DARPA BioMagnetics Grant
"Synthesis and Magnetic Properties of Au-Coated Amorphous $Fe_{20}Ni_{80}$ Nanoparticles,"

2) B.L. Cushing, V. Golub, and C.J. O'Connor, J. Phys. Chem. Solids, 65(4), 2004, 825-829.

3) "Nanocomposites based on semiconductor and magnetic nanocrystals: fabrication and characterization," Lifang Shi, Deshang Wang, Liane Rossi, Yuri Barnakov and Zeev Rosenzweig, Proc. SPIE (2004) Vol. 5593, p. 317-328, Nanosensing: Materials and Devices; (M. Saif Islam, Achyut K. Dutta; Eds.)

4) "Synthesis of Variable-Sized Nanocrystals of Fe_3O_4 with High Surface Reactivity," D. Caruntu, G. Caruntu, Y. Chen, C.J. O'Connor, G. Goloverda, and V.L. Kolesnichenko, Chem. Mater., 16(25), 2004, 5527-5534.

5) "Drug-Loaded, Magnetic, Hollow Silica Nanocomposites for Nanomedicine," W. Zhou, P. Gao, L. Shao, D. Caruntu, M. Yu, J. Chen, and C.J. O'Connor, Nanomedicine, 1(3), 2005, 233-237.

6) "Attachment of Gold Nanograins onto Colloidal Magnetite Nanocrystals," D. Caruntu, B.L. Cushing, G. Caruntu, C.J. O'Connor, Chem. Mater., 17, 2005, 3398-3402.

7) "Effects of Annealing on the Magnetic Properties, Size and Strain of Gold-Coated Permalloy Nanoparticles," B.L Cushing, V.O. Golub, M. Henry, B.L. Oliva, E. Cook, C.W. Holmes, and C.J. O'Connor, 0Nanotechnol., 16, 2005, 1701-1706.

8) "Structure-Release Rate Correlation in Collagen Gels Containing Fluorescent Drug Analogs," LaCerda, S. D.; Ingber B.; Rosenzweig, N.; Biomaterials 2005 26(34), 7164-7172.

9) "Manipulation of the Magnetic Properties of Magnetite-Silica Nanocomposite Materials by Controlled Stober Synthesis," Barnakov, Y. A.; Yu, M. H.; Rosenzweig, Z.; Langmuir; 2005; 21(16); 7524-7527

10) "Fabrication of Magnetic Hollow Silica Nanospheres for Bioapplications," L. Shao, D. Caruntu, J.F. Chen, C.J. O'Connor, and W.L. Zhou, J. Appl. Phys. 97, 2005, 10Q908-10Q908-3.

11) "Magnetic Hollow Silica Nanotubes for Bio-applications," P. Gao; D. Caruntu, L. Shao, M. Yu, J.F. Chen, C.J. O'Connor, W.L. Zhou, Magnetics Conference, 2005. INTERMAG Asia 2005. Digests of the IEEE International, 4-8 April 2005 Page(s):801 – 802.

12) “Structure-Release Rate Correlation in Collagen Gels Containing Fluorescent Drug Analog,” Silvia De Paoli Lacerda, Bruce Ingber, Nitsa Rosenzweig, Biomaterials Vol. 26 pp. 7164-7172 (2005).

13) “One-step Synthesis of Magnetic Hollow Silica and Their Application for Nanomedicine,” W. Wu, M.A. DeCoster, B.M. Daniel, J.F. Chen, M.H. Yu, D. Caruntu,

14) “Magnetic modulation of drug release from magnetic collagen hydrogels,” C.J. O'Connor, and W.L. Zhou, J. Appl. Phys., 99(8), 2006, 08H104/1-08H104/3.

15) Vania M. De Paoli[1], Silvia H. De Paoli Lacerdi[1], Bruce Ingber[2], Zeev Rosenzweig[1] and Nitsa Rosenzweig,[1*] Accepted for publication Langmuir (January 2006).

16) “One Pot Synthesis of Nearly Monodisperse Magnetic Nanoparticles,” G. Caruntu, A. Newell, D. Caruntu, C’J. O’Connor, submitted to Chem. Mater. May 2006

17) “Formation of Gold-Coated Magnetic Nanoparticles using TiO2 as a Bridging Material,” B.L. Oliva, A. Pradhan, D. Caruntu, C.J. O'Connor, and M.A. Tarr, J. Mater. Res., 21(5), 2006, 1312-1316.

“18) Superparamagnetic Resonance Spectra of de novo Biomagnetic Materials,” Larisa Radu, Michelle White, Daniella Caruntu, John Wiley, Charles J. O’Connor, Paul Hanson, Journal of Experimental Nanoscience, 2006, in press

19) “Synthesis of Magnetic Hollow Silica using Polystyrene Bead as a Template,” W. Wu, D. Caruntu, A. Martin, M.H. Yu, C.J. O’Connor, W.L. Zhou, and J.-F. Chen, J. Magn. Magn. Mater., 311, 2007, 578–582.

20) “One-Pot Synthesis of Highly Crystalline and Monodisperse Hydrophobic MFe_2O_4 (M=Mn, Fe, Co, Zn) Nanocrystals,” Caruntu, G.; Newell, A., Caruntu, D., O’Connor, C. J., submitted to Chemistry of Materials (August 2006)

21) “Synthesis and Application of Quantum Dots FRET–Based Protease Sensors,” Lifang Shi, Vania de Paoli, Nitsa Rosenzweig and Zeev Rosenzweig, JACS Published on web 07.26.2006

22) “Fluorescence–based Zinc Ion Sensor for Zinc Ion Release from Pancreatic Cells,” Georgeta Crivat, Kazuya Kikuchi, Tetsuo Nagano, Tsvia Priel, Michal Hershfinkel, Israel Sekler, Nitsa Rosenzweig and Zeev Rosenzweig, Anal. Chem. 2006 Published on web 07.18.2006

23) “Quantum Dots FRET Probes Discriminate Between Normal and Cancerous Breast Cells,” Lifang Shi, Vania de Paoli, Nitsa Rosenzweig and Zeev Rosenzweig, Submitted to Anal. Chem. July 2006

24) “Magnetic modulation of drug release from magnetic collagen hydrogels,” Vania M. De Paoli, Silvia H. De Paoli Lacerdi, Bruce Ingber, Brian Cushing and Nitsa Rosenzweig, Langmuir Published on web 05.13.2006

25) “Poly(allylamine) Stabilized Iron Oxide Magnetic Nanoparticles,” J.M. El Khoury, D. Caruntu, C.J. O'Connor, K.-U. Jeong, S.Z.D. Cheng, and J. Hu, J. Nanoparticle Research, 9(5), 2007, 959-964.

26) “Fluorescent Silica Nanospheres for Digital Counting Bioassay of the Breast Cancer Marker HER2/nue,” Liane M. Rossi[b], Lifang Shi[a] , Nitsa Rosenzweig[a] and Zeev Rosenzweig,[a]* Biosensors and Bioelectronics (in press).

AMRI Presentations 2004-07 – DARPA BioMagnetics Grant

“Drug-Containing Nanoparticles – New Strategies for Cancer Chemotherapy,” Silvia De Paoli Lacerda, Li Chen, Zeev Rosenzweig, Nitsa Rosenzweig, Interdisciplinary Cancer Research Workshop University of New Orleans, November 2004.

“Localization & Controlled Release of Chemotherapeutic Drugs Using Oscillating Magnetic Field (OMF),” Nitsa Rosenzweig Louisiana Breast Cancer Task Force, 13th Annual Meeting, Mandeville, LA, May 14, 2005

“Collagen-Based Drug Delivery System for Controlled Release of Chemotherapeutic Drugs in Breast Cancer Treatment,” Silvia De Paoli Lacerda, Bruce F. Ingber, Nitsa Rosenzweig, 2nd Annual Tulane Women’s Health Research Marathon Day, New Orleans, LA, May 16, 2005

“Silica-Coated Magnetic Particles for Bio-separation,” Lifang Shi and Zeev Rosenzweig, Pittcon 2005, Orlando Florida, March 2005.

“Magnetic Hollow Silica Nanostructures for Nanomedicine Application,” W.L. Zhou, P. Gao, D. Caruntu, L. Shao, M.H. Yu, J.F. Chen, and C.J. O’Connor, Beijing International Nano Conference, June 8-11, 2005, Beijing, China.

“Magnetic Hollow Silica Nanostructures”, W.L. Zhou, P. Gao, D. Caruntu, L. Shao, M.H. Yu, J.F. Chen, and C.J. O’Connor, July31- Aug.4, 2005, Honolulu, Hawaii.

“Manipulation of Pore Size of Hollow Silica for Nanomedicine Application,” Angela Martin, Wei Wu, and Weilie L. Zhou, International Congress of Nanotechnology, Oct.31-Nov.3, San Francisco, 2005

“One Step Synthesis of Magnetic Hollow Silica and Their Application for Nanomedicine,” W. Wu, M.A. DeCoster, B.M. Daniel, J.F. Chen, M.H. Yu, D. Cruntu, C.J. O’Connor, and W.L. Zhou, 50th Magnetism and Magnetic Materials Conference, Oct.30-Nov.3, San Jose, California, 2005.

"Characterization and photocatalytic activity of magnetite-titania-gold nanocomposite materials," Anindya Pradhan, Brittany L. Oliva, Daniela Caruntu, Charles J. O'Connor, and Matthew A. Tarr, ACS National Meeting, Atlanta, March 2006.

"Formation and characterization of magnetite-titania-gold nanocomposite materials," Brittany L. Oliva, Anindya Pradhan, Daniela Caruntu, Charles J. O'Connor, and Matthew A. Tarr, ACS National Meeting, Atlanta, March 2006.

"Superparamagnetic Resonance Spectra of *de novo* Biomagnetic Materials," Larisa Radu, Monica Concha, Sara DeLong, Daniella Caruntu, Challa Kumar, John Wiley, Charles J. O'Connor, Paul Hanson –July, 2006, IEEE Nano-2006, Cincinnati, OH

"Superparamagnetic Resonance Spectra of *de novo* Biomagnetic Materials," Larisa Radu, Michelle White, Daniella Caruntu, John Wiley, Charles J. O'Connor, Paul Hanson –May, 2006, 2006 NSTI Nanotechnology meeting, Boston, MA

"Ligand-dependent Changes in the EPR Spectra of Magnetite Nanoparticles," Larisa Radu, Michelle White, Daniella Caruntu, John Wiley, Charles J. O'Connor, Paul Hanson – April, 2006 at the 3rd Annual Foundations of Nanoscience: Self-Assembled Nanostructures and Devices, Snowbird, Utah

"Synthesis of Ibuprofen Loaded Magnetic Solid Lipid Nanoparticles," Xiujuan. Pang, Jiajun.Chen, Jie Zhou, Minghui Yu, Fude Cui, and Weilie Zhou, Submitted to 10th Joint Intermag Conference, Baltimore, Jan.7-12 (2007).

Future Research

This brief technical report demonstrates the successful development of synthetic techniques for the preparation of magnetic nanoparticles and nanocomposites. The new synthetic techniques greatly enhance our ability to control the size, size distribution, and surface and bulk chemical and physical properties of nanoparticles in general and magnetic nanoparticles in particular. Few challenges remain even as the Biomagnetics project comes to an end. The first and foremost challenge is in the ability to scale up the synthesis to the mg and g quantities. In our laboratories we are only able to produce smaller quantities of materials. Their long term stability has also been a problem. Solving this problem will require the involvement of chemical engineers who will design and construct a pilot system to produce large quantities of magnetic nanomaterials while maintaining their unique properties as they are formed in the laboratory. The potential impact of nanomaterials on the environment and on human health is also a challenge. At this time, the information we have is not sufficient to make decisions whether to mass

produce magnetic nanocomposite particles or not. More studies are needed in this area to assess the toxicity properties of these materials. One cannot ignore however their great potential to transform fields like drug delivery and clinical diagnostics. Studies will continue in the next decade to further establish magnetic nanoparticles and nanocomposites as viable imaging and probing tools in biological systems and as transformative drug delivery carriers which hold promise to improve human health.

PART 2 – LSU-CAMD Report

Development of Magnetic Nanomaterials and Devices for Biological Applications

DARPA Grant No. HR0011-04-C-0068

(Subcontractor: LSU/CAMD)
Center for Advanced Microstructures and Devices
Louisiana State University
6980 Jefferson Hwy. Baton Rouge, LA70806

Development of Magnetic Nanomaterials and Devices for Biological Applications

Prime Contract to UNO from Defense Advanced Research Projects Agency (DARPA) Prime Contract Number HR0011-04-C-0068, CAMD Subcontract Number 04-085-S1

Final Report

October 2007

Editors: Jost Goettert, Challa Kumar

Center for Advanced Microstructures and Devices, Louisiana State University
6980 Jefferson Hwy. Baton Rouge, LA70806

Summary

In support of DARPA's overall goal to develop a handheld Bio-Sensor using GMR detection of bio-functionalized magnetic nanoparticles, CAMD researchers contributed to two major tasks related to (1) the fabrication, assembly, integration and testing of GMR sensors integrated into microfluidic systems and (2) the synthesis and characterization of bio-functionalized magnetic nanoparticles. This final report briefly summarizes the main research accomplishments with further details of efforts and results available from our semi-annual reports submitted in the past.

Figure 1 illustrates our two main efforts in relation to the overall project goal. Two critical aspects essential to achieve the overall goal are the integration of silicon based GMR magnetic sensor chips into microfluidic platforms including bio-functionalized surface modification, and the synthesis of dedicated magnetic nanoparticles with surface properties enabling the detection of selective bio-species. The report is listing main results of each effort in separate sections.

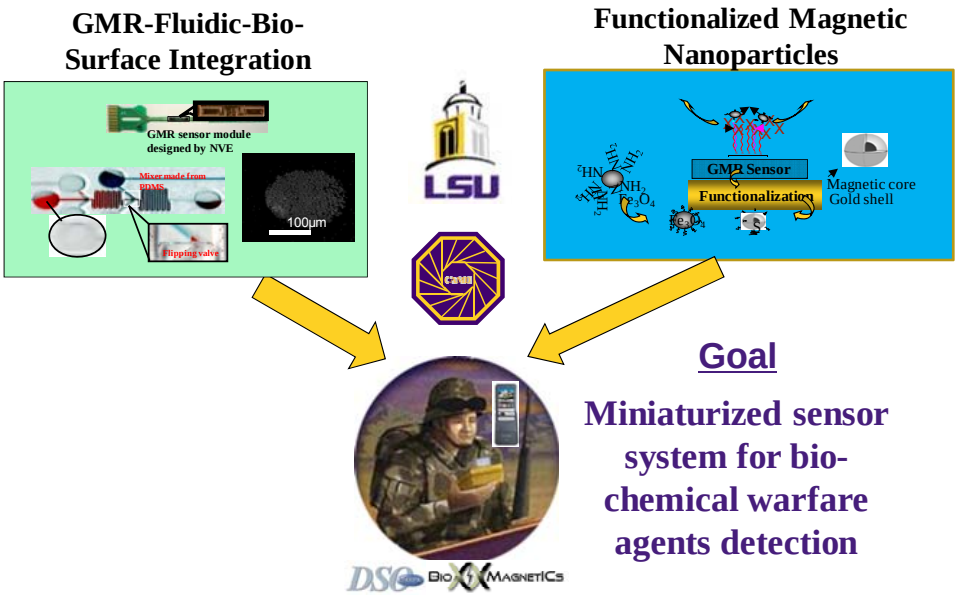

Fig. 1: Overview of CAMD research focus within the DARPA Bio-Magnetics project.

1. Sensor System Fabrication and Integration

Figure 2 shows the main tasks associated with the integration of GMR sensor chips into polymer microfluidic handling system including surface bio-functionalization to selective bind functionalized magnetic nanoparticles.

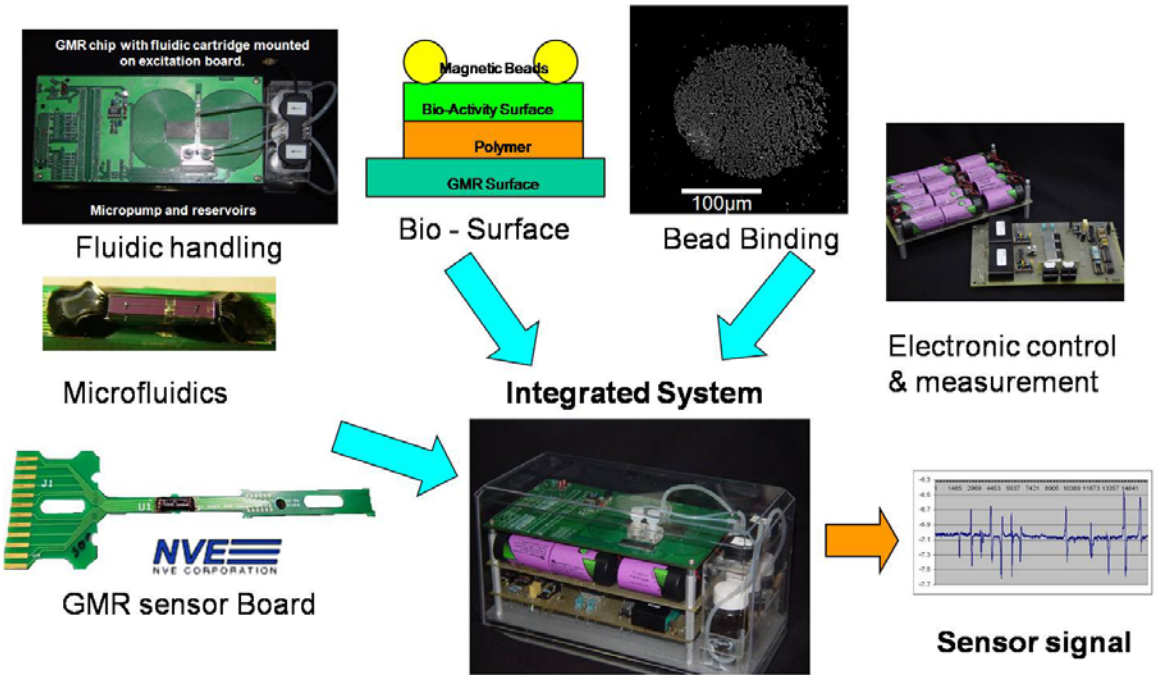

Fig. 2: Major CAMD tasks associated with fabrication and integration of the Magnetic Biosensor.

The GMR sensor chips were provided by NVE Corporation (also partner and sub-contractor in this DARPA program) in a pre-assembled form mounted on a special PCB board (so-called diving board). The sensor surface is protected by a thin Si_3N_4 film ensuring that the sensors were not shortened when fluidic was pushed across the surface. This surface film is also the interface for the bio-functionalization chemistry.

a. Fluidic Cartridge for GMR sensors

Microfluidic channels were patterned on top of the GMR sensors using an aligned optical lithography process in SU-8 resist. Channels with lateral dimensions down to10µm and up to 50µm tall have been patterned and successfully sealed with an SU-8 film using a novel process called semi-solid transfer. An additional SU-8 layer is providing relatively large (0.5mm diameter) inlet and outlet structures interfacing the chip with a fluidic cartridge. The SU-8 lithography process was done on a wafer-scale producing nearly 1000 GMR sensor dices in a parallel fabrication process. After wafer dicing the individual sensor chips were mounted onto the electronic diving board and electrically connected via wire-bonding. The diving board mounted sensors were interfaced with a fluidic cartridge that provided a robust and user-friendly macroscopic fluidic interface using standard fluid connectors. This setting enables researcher to easily mount the diving board onto the excitation board and run fluids across the GMR surface in a well-defined manner. Figures 3 show some results.

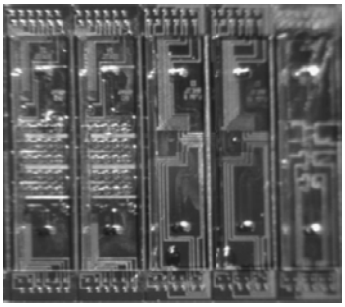

5 sensor dices with added fluidic microchannels on a full 4" wafer.

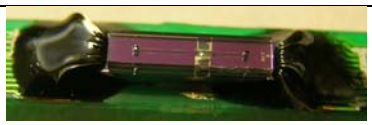

GMR chip with microfluidic structure mounted onto diving board and wire-bond connected. The wires are protected with epoxy glue.

Fluidic cartridge providing an interface between microfluidic channels and macroscopic fluidic connectors.

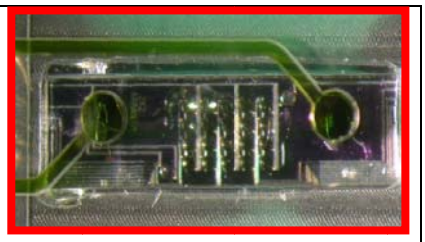

Microfluidic inlet/outlet with channel system patterned on GMR chip (wafer-scale) using optical lithography. Colored water proves no leak.

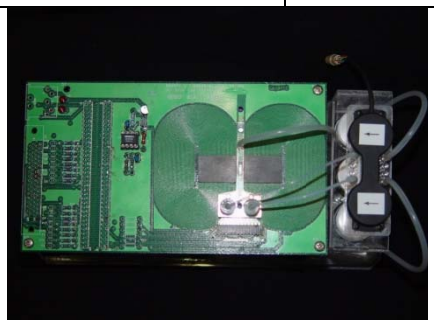

GMR sensor with fluidic cartridge mounted onto magnetic excitation board and connected to fluidic reservoirs with ferrofluid and oil samples.

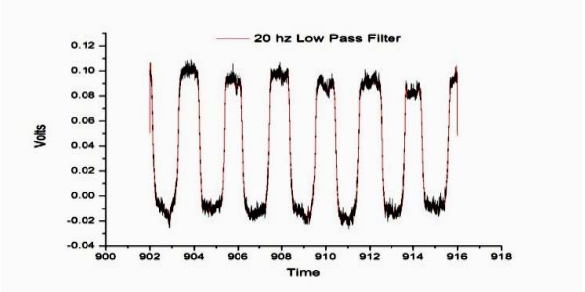

Ferrofluid/oil plugs pumped into the cartridge and the microfluidic channels generating a GMR signal when the ferrofluid is passing across the sensor surface.

Figs. 3: Steps in the fabrication and testing procedure of GMR-microfluidic chips.

This integration approach combines GMR silicon sensor chips with micro-macrofluidic handling systems delivering a 'hard' plastic structure with superior fluid flow control. Additional attributes are

(+) Lithographically defined microfluidic structures with smallest features down to 10µm and heights up to 50 µm will allow guiding fluidic samples even to very small sensor chips;

(+) Lithographically defined micro-macrofluidic interface enabling relatively simple connection to fluidic reservoirs and fluid operation using a custom-made, re-usable cartridge;

(+) Microfluidic structures are batch processed using aligned optical lithography on a pre-structured GMR sensor silicon wafer enabling a cost-effective, large-scale fabrication of GMR sensor chips with added microchannels;

(-) Microfluidic channels are sealed with the same hard-plastic material (SU-8) providing a uniform environment for the fluid.

b. Vertical Microfluidic Development Platform

In order to allow simple access to the GMR surface (surface functionalization, visual inspection of surface chemistry after an experiment, taking surface samples) an alternative concept based on a microfluidic platform has been developed utilizing molded polymer fluidic chips vertically stacked in a frame that provides electrical, optical, and macrofluidic interface

features. This stack is sequentially assembled allowing to modifying GMR sensor surfaces with bio-functionalized coatings prior to completely assemble the device. The stack concept is illustrated in Fig. 4 with Figs. 5 showing some examples of fluidic chips and experiments.

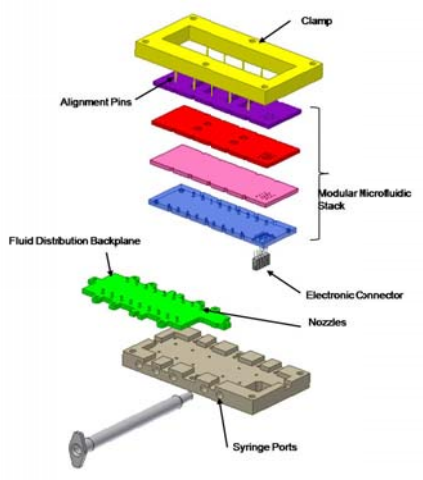

Fig. 4: Schematic of vertical stack assembly.The stack uses standard polymer chips 1" x 3"(glass slide format).

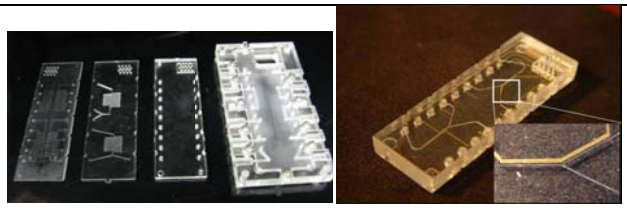

Distribution plate and different fluidic chips after fabrication and prior to assembly (left). Fluidic chip with conductive wire pattern for bead manipulation and electrical detection (right).

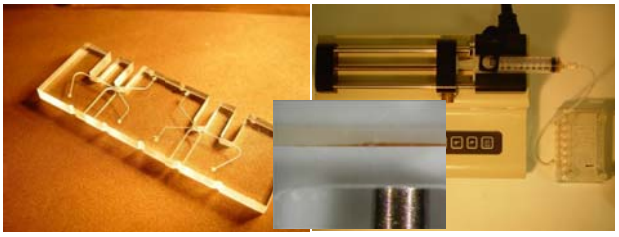

Magnetic pre-concentrator chip with fluidic y-junction (left) and bead concentration measurement (right, insert).

Fig.5:Example of stack compatible fluidic chips

A base plate provides simple access ports for example to syringe pumps. A fluid backplane connects these fluid inputs to dedicated ports inside the microfluidic stack routing the chemicals into the appropriate microchannels. At this time CAMD has started building a library of dedicated chips designed for specific functions including fluidic mixing, magnetic separation, GMR sensing, and optical inspection. Each chip function can be tested individually or in an arbitrary combination due to the use of standardized microfluidic interconnects. Chip stacking uses the concept of elastic averaging to passively align polymer chips (typically made from PMMA and PC) in an easy, user-friendly fashion. Chips are molded using hot embossing and are either sealed permanently with a thermo-welding process or temporarily using a soft gasket. The gasket also offers the opportunity to disassemble the stack after completing the experiments and closely investigate the surface.

The stack allows the convenient use of microfluidic designs and solutions in a fast, cost-effective way. The modular approach using a simple assembly process is highly flexible and can easily accommodate user needs. A drawback is the limited smallest size of fluidic channels (typically about 100µm) determined by the fabrication process which uses a combination of precision micromachining and molding. Using a LIGA fabrication approach, however, a mold insert with smaller dimensions will be possible to fabricate.

c. GMR Surface Functionalization

Surface functionalization of GMR chips with a thin layer of biomolecules which allows selective binding or target molecules is typically an add-on process, for example using spotting. However, complex procedures had to be developed to optimize bonding selectivity and optimize signal-to-noise ratios. The fluidic stack was successfully utilized for systematic studies of bio-functionalized surfaces and their preparation. In addition, executing the bio-protocol - a specific fluidic procedure with different chemicals required to activating the surface, reacting the sample molecules, removing any unwanted, non-specifically bound molecules through washing, and

finally detecting the sample - in a microfluidic environment resembling the actual sensor dimension is accelerating the development dramatically and will allow quick transition from basic research to sensor prototype devices. Figs. 6 show as an example a test chip containing up to 10 GMR chips treated with different surface chemistry and undergoing the identical bio-protocol. It should be noted that these tests used fluorescent-labeled nanoparticles instead of magnetic labels due to problems with the electronic signal stability.

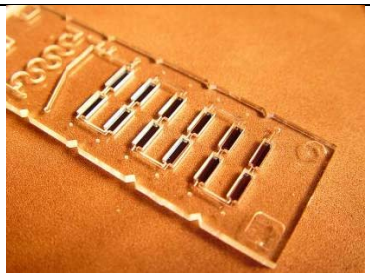

Fluidic test chip with 10 GMR chips prepared with different surface coatings for screening tests.

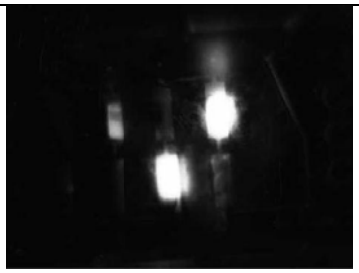

Chemi-luminescent signal from captured molecules from different chips on a light sensitive film

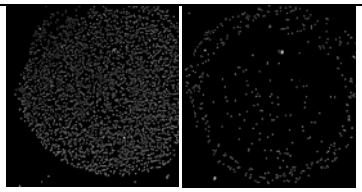

Photographs of bound beads (3µm Dynabeads) on a 200µm diameter spotted surface. Passivation of the outside area reduces the non-selective binding of the beads and thus increases signal-to-noise ratio.

Figs. 6: Use of fluidic chips and stack assembly for systematic studies of bio-functionalized surfaces on GMR sensor chips.

In conclusion the flexibility and simplicity of the fluidic stack development platform makes it an ideal research tool not only for this sensor project but for a number of other projects and life science applications currently being investigated. Continuously using this platform will increase the number of fluidic chips available for a particular experiment and will accelerate using microfluidic solutions in a wide range of life science applications including cell analysis, protein crystal growth, sensor chips for optical detection of bound bio-molecules, and microreactor based synthesis of specialty chemicals, in particular nanoparticles.

d. Summary Sensor System Fabrication and Integration

The GMR-microfluidic integration efforts are still work in progress and haven't resulted in a stable solution and a handheld Bio-Sensor device suitable for serious testing. The following table provides some key lessons learned that may guide future research efforts:

- The pre-defined GMR electronic package (diving board, excitation) is a very strict boundary condition for integrating a microfluidic system; alternative, more rigid solutions might be possible starting with the naked silicon chip directly embedded into the polymer chips or using more reliable platforms such as DIP IC chip carrier.
- Vertical fluidic development platform is an enabling research tool giving users a microfluidic handling system with convenient interface features to standard laboratory equipment such as syringe pumps, pipettes, fluorescent microscopes, and similar; there is already a set of designs for basic fluidic functions available that can be easily extended to new, customer-defined chip designs further supporting its use in life science applications.
- Bio-functionalization of the GMR sensor surface is an important issue and significantly compromises MEMS fabrication and ultimately sensor fabrication costs; while flow sensing applications (for example detecting beads passing across the surface) are feasible bio-sensing may require alternative approaches decoupling the actual bio-reaction from the GMR signal generation.
- Use of magnetic forces to 'manipulate' bead loaded liquid flow is an interesting concept and should be further explored within the stack confinement for basic fluid processing operations such as mixing, pre-concentrating, and re-directing.

2. Development of Magnetic Nanoparticles for GMR Bio-Sensors

Magnetic nanoparticles with high magnetic moment are a key component to improve the sensitivity of GMR detection. In addition to the magnetic moment, enhancement of magnetic properties such as blocking temperature, coercivity, and saturation magnetization of the magnetic nanoparticles is also required. Magnetic properties of the nanoparticles are strongly influenced by the presence of organic as well as inorganic protective shells on their surface. Taking advantage of this, we have begun a systematic investigation to design new cobalt-based magnetic nanoparticles with improved magnetic properties by varying the magnetic core and its size, and adding a protective metallic shell with varying thickness and the chemical nature of the stabilizing agent. In addition, we have also investigated the approaches to bio-functionalization of planar surfaces and fundamental aspects of magnetic nanoparticle formation in order to control the properties of magnetic nanoparticles by controlling their formation at molecular level. The investigations from the whole project can be broadly classified into the following three categories.

a. Biofunctionalization of Gold Surfaces with Magnetic Nanoparticles

We synthesized streptavidin-functionalized magnetic nanoparticles and characterized their binding to biotinylated SAMs (self assembled monolayers) on gold for biological recognition applications. Magnetic nanoparticles (Fe3O4) were prepared by co-precipitating Fe^{+2} and Fe^{+3} ions by ammonia solution. They were conjugated to streptavidin. The gold surface was functionalized with biotin-HPDP. The thiol-capped biotin immobilized on gold was able to capture the streptavidin-conjugated nanoparticles as demonstrated by SEM images that show particles that remain after washing. The size of the functionalized particles was not uniform due to some clumping nature. The EDS analysis confirmed the presence of nanoparticles on the biotinylated gold surface as well. The intensity of EDS signal is directly proportional to the size of the particle that is confirmed by the increase in the intensity of iron signal as the particle's size increases. FT-IR spectra and fluorescent images also confirmed the nanoparticle capture on biotinylated gold surface, albeit with less resolution. For more details on this topic see: Bala G. Nidumolu, Michelle C. Urbina, Josef Hormes, Challa S. S. R. Kumar, and W. Todd Monroe**, Functionalization of Gold and Glass Surfaces with Magnetic Nanoparticles Using Biomolecular Interactions,** *Biotechnology Progress*, 22(1), 91-95, 2006.

b. Magnetic-polymer Nanocomposites

The synthesis of iron - PMMA composite nanoparticles was carried out mainly by the ex-situ method, i.e, by dispersing the synthesized magnetic nanoparticle into organic PMMA solvents or by polymerization of methylmethacrylate monomer in the presence of the magnetic nanoparticles. Recently, in-situ synthesis of magnetic polymeric nanocomposites by a high-temperature thermal or high-intensity ultra-sonochemical decomposition method was reported. We have developed a simple room-temperature synthesis of PMMA stabilized iron tetrahydrofuran (THF) colloidal nanoparticle from iron (II) chloride with superhydride as reducing agent under ultrasonic stirring condition. These colloidal nanoparticles can be easily solidification into PMMA magnetic nanocomposites in many kinds of molds for microfabrication under the ultrasonic stirring condition during solvent evaporation. The body-center cubic (bcc or α) phase structure and zero-valence state of iron nanoparticles was proved by selected area electron diffraction (SAED) and X-ray absorption near-edge structure (XANES) spectroscopy. The magnetic properties for these PMMA stabilized iron nanoparticles were also investigated.

c. Magnetic Core-metal Shell Nanoparticles

The ferromagnetic cobalt-core gold-shell nanoparticles (size 2.7 nm ± 0.5 nm) were synthesized using a displacement reaction in THF. The nanoparticles were embedded within polymeric nanoshells, made up of anionic polyelectrolyte layers, of 5 μm diameter microcapsules using layer-by layer assembly technique. Application of an oscillating electromagnet with frequency of 100~300 Hz and field strength of 120 Oe to the microcapsules modifies the capsule wall structure leading to an increase in macromolecules permeability in to the microcapsules. More details are described in: Zonghuan Lu, Malcolm D. Prouty, Zhanhu Gao, Vladimir O. Golub, Challa S.S.R. Kumar, Yuri M. Lvov, **Magnetic Switch of Permeability for Polyelectrolyte Microcapsules Embedded with Co@Au Nanoparticles**, *Langmuir*, 21(5), 2042 -2050, **2005**.

An alternative preparation of Co@Au nanoparticles with three different Co core size and similar Au shell thickness is using a conventional 'flask process' utilizing adisplacement process. The Co@Au particles with different core sizes were characterized using XANES and SQUID magnetometer. In addition to the traditional "flask process," the research was also focused on developing a three step process to generate bio-functionalized cobalt (Co)-core gold (Au)-shell nanoparticles using polymer microreactor process technology. The continuous generation of the bio-functionalized core shell nanoparticles using a microfluidic reactor system will ultimately lead to a large scale continuous production of bio-functionalized Co@Au nanoparticles with superior control of critical properties like particle size and size distribution.

In addition to reproducing the reported high temperature procedures for preparation of cobalt gold shell nanoparticles, we have developed our own room temperature process for synthesis of biotinylated cobalt core gold shell nanoparticles. All steps are performed using standard laboratory glass ware at room temperature under ultrasonication. In the first step, cobalt (II) chloride is reduced by lithium hydrotriethylborate ($LiHBEt_3$) in tetrahydrofuran (THF). The cobalt core formation is controlled by the surfactant (SB3-12). In the second step water-free hydrogen tetrachloroaurate(III) is reduced on the cobalt core based on redox process followed by formation of gold atoms directly through reduction of Au(III). This gold shell is formed in THF with $LiHBEt_3$ and stabilized by SB3-12. The particles are well washed in ethanol and dried. In the last step the surfactant (SB3-12) is replaced by biotin. Biotin is bound to the gold surface via a thiol group. As seen in the above figure, the biotinylated Co@Au nanoparticles have an average diameter of 4.3 nm. They have also been found to be stable in air and acidic conditions. They have been found to retain their magnetic properties even after keeping them one month in diluted acid (HCl 8%).

d. Improving the Magnetic Properties of Co-nanoparticles through Mechanistic Investigations

i) Mechanistic Investigation of the Precursor Effect

We have also embarked on a project to identify alternative organo-metallic cobalt complexes from which cobalt nanoparticles can be prepared. It is worth emphasizing that except for the organometallic cobalt precursors such as $[Co(\eta^3\text{-}C_8H_{13})(\eta^4\text{-}C_8H_{12})]$ and $[Co_2(CO)_8]$, no other organo-metallic cobalt complexes have been explored until now for the synthesis of cobalt nanoparticles. It seemed of interest to investigate also the precursor effect on the size, shape, electronic, geometric and magnetic properties of cobalt NPs. We obtained cobalt NPs from thermal decomposition of the new organo-metallic complex (RDS-5) and compared these to Co NPs obtained with well known $[Co_2(CO)_8]$ under identical reaction conditions. Results obtained so far showed as a surprising result that Co NPs obtained from the new complex have different magnetic properties. We are in the process filing a technology disclosure to protect this invention. NPs prepared from [RDS-5] and $[Co_2(CO)_8]$ show blocking temperatures T_B = 170 K and 30 K, coercive field of 1577 Oe and 533 Oe, respectively.

We have also observed a 'precursor effect' on the physical and chemical properties of the obtained cobalt nanoparticles. We have isolated the reaction intermediate that is observed during the formation of cobalt nanoparticles from the new precursor, an alkyne-bridged dicobalt hexacarbonyl compound [(Co_2(μ-HC≡CH)$(CO)_6$] (RDS-5). The intermediate compound was identified as the tricyclic organocobalt complex, [$Co_3(CO)_9CCH_3$] based on characterization using IR and X-ray crystallographic analysis. Suitable crystals for the X-ray diffraction analysis were grown as dark red plates from a saturated hexane solution of [$Co_3(CO)_9CCH_3$] at 4 ºC. The structure was determined using diffraction data collected at 150K using graphite monochromated MoKα radiation on a Nonius Kappa CCD diffractometer. *Crystal data*: triclinic, space group P-1, a = 7.7450(10), b = 8.7295(11), c =12.1758(15) Å, α = 86.927(8), β = 82.201(6), γ = 67.662(7)°, V = 754.39(16) $Å^3$, Z = 2, μ(MoKα) = 3.30mm^{-1}, 25541 reflections collected with θ<36.3°, 7061 unique, R_{int} = 0.027; R = 0.040, wR_2 = 0.113, refined on F^2. Co-Co distances are in the range 2.4669(4) – 2.4770(5) Å. The crystals are destroyed by an apparent phase change at lower temperatures. The molecular structure of this complex is shown in the figure below together with the atomic numbering scheme. The intermediate is different from $Co_4(CO)_{12}$ that is reported in the case of the decomposition of the well known [$Co_2(CO)_8$] (DCO) complex.

The TEM micrographs of cobalt NPs obtained from [$Co_2(CO)_8$] as precursor from particles when no more CO was detected in the IR spectrum (a) and the final product after 30 min (b). Similar TEM pictures for [(Co_2(μ-HC≡CH)$(CO)_6$] are given in (c) and (d), respectively. By comparing Figs (a) and (b) and (c) and (d) respectively one can see that particle sizes still change after the complete use of the precursor molecules monitored by the CO content. The size distributions of the final products for DCO and ADH are shown in the figures (e) and (f), respectively. Particles obtained from ADH are significantly larger (about 6 nm) compared with those from DCO (about 3 nm) using identical reaction parameters. The synthesized Co-nanoparticles are not yet monodisperse and both size distributions are still quite broad.

The Co nanoparticles obtained from both precursors (ADH & DCO) were also exposed to atmospheric conditions and their air stability was monitored using Co-K edge XANES spectroscopy. The Co-K-XANES spectra of the nanoparticles as synthesized are compared with spectra of the particles exposed to air for either 2 weeks (ADH and DCO) or 1 month (ADH), and with the spectrum of CoO, the expected oxidation product of the nanoparticles. The oxidized spectra were fitted by using the spectra of CoO and the as synthesized particles as basis set. Also these fits are shown in the respective figures. The fits show that already 84% of the particles from the DCO synthesis are oxidized as compared to just 34% for the particles from ADH. Even after one month of exposure to air just about 50% of the particles from ADH are oxidized showing clearly the higher stability of particles from ADH against oxidation as compared to those from DCO. For more information, see our publication : Rohini DeSilva, Vadim Palshin, Frank R Fronczek, Josef Hormes and Challa SSR Kumar, **Investigation of the Influence of Organometallic Precursors on the Formation of Cobalt Nanoparticles**, *J. Phys. Chem C.*, 111(28), 10320-10328, 2007.

ii) Mechanistic Investigation of the Influence of Surfactants on Cobalt Nanoparticle Formation

We have also carried out investigations into the mechanism of formation of cobalt nanoparticles obtained from the decomposition of organometallic precursor, alkyne-bridged dicobalt hexacarbonyl, (ADH) and the influence of various surfactants on the reaction path way, delineated using time dependent FT-IR spectroscopy. The intermediates formed were characterized using FT-IR analysis and the likely presence of highly unstable species in the reaction pathway was supported by theoretical calculations. Similar reaction intermediates and pathways, albeit with disimilar kinetics, were noticed in the presence of oleic acid and octadecyl amine(ODA). The utilization of less basic surfactant like trioctylphopshine oxide (TOPO) led to

different reaction pathway and reaction intermediates leading to the formation of Co nanoparticles. On the other hand, strong basic surfactants like trioctylphosphine (TOP) appear to actively coordinate to the precursor from the very beginning to produce yet another set of reaction intermediates and a new reaction pathway. The effect of surfactants on the reaction pathway and reaction intermediates was in turn seen on the crystal structure, particle size, size distribution and magnetic properties of the cobalt nanoparticles obtained. Crystal structure of the cobalt nanoparticles was determined using synchrotron radiation based X-ray absorption spectroscopy (XAS). Particles size and size distribution was obtained from Transmission Electron Microscopy (TEM) and the magnetic properties were measured using SQUID magnetometry.

A novel cobalt Single Molecule Magnet (SMM) ([Co(Cp)2]2[CoCl4]), whose chemical formula is $Co_2C_{10}H_{10}C_{l4}$, has been obtained as shown in the synthetic scheme below (Fig. 7). The new Co SMM has higher blocking temperature (>10 k) compared to other cobalt based SMMs. It is soluble in both aqueous and organic solvents. Its optical properties are solvent dependent. It has cobalt in two oxidation states leading to potential electrochemical applications. A technology disclosure has been filed based on this discovery.

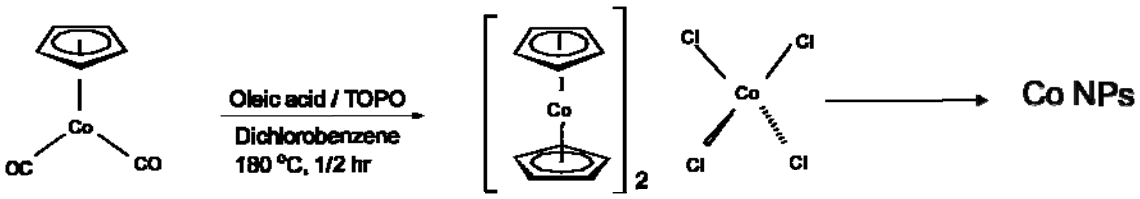

Fig. 7: Reaction scheme of a novel Co single Molecule Magnet.

The magnetic properties of the cobalt nanoparticles obtained using oleic acid alone as the surfactant were determined. The temperature dependence of magnetization was measured in an applied magnetic field of 100 Oe between 2 and 300 K using zero-field-cooling (ZFC) and field-cooling procedure. It evidences a typical super paramagnetic behavior with blocking temperatures T_B = 170 K and 30 K for the NPs prepared from ADH and DCO respectively. They show no hysteresis in their magnetization data at 300 K, indicating a superparamagnetism at room temperature. At 10 K, the NPs from ADH shows a larger coercive field of 1577 Oe compared to the NPs with only 533 Oe.

In addition, we have utilized the same precursors and prepared cobalt nanoparticles under identical conditions by utilizing a mixture of oleic acid and trioctyl phosphine as surfactants. The behavior of the two precursors in the presence of both oleic acid and TOP is very different to that of the behavior observed in reactions with oleic acid alone as seen from the time dependent FT-IR spectra. It is very likely that since the surfactant TOP is a strong base and its lone pair can easily be coordinated to cobalt atoms, it may be playing a major role in cobalt nanoparticle formation.

The cobalt nanoparticles, obtained from both the precursors when TOP and oleic acid are used as surfactants, were also found to have similar particle sizes, size distributions and magnetic properties. A detailed X-ray absorption spectroscopy investigation of the geometric and electronic properties as well as magnetic properties of the cobalt nanoparticles is currently in progress. These investigations clearly demonstrate the important role reaction intermediates can play in controlling the formation and in the properties of cobalt nanoparticles. For more information on these investigations see our publication that will be appearing in Journal of Materials Chemistry (2008).

e. Summary Development of Magnetic Nanoparticles for GMR Bio-Sensors

In conclusion, our investigations related to the design and development of novel magnetic nanoparticles have led to the following:

- The magnetic properties of nanoparticles can be fine-tuned by varying the dimensions and nature of magnetic core-shell architecture.
- Understanding the mechanism of magnetic nanoparticle formation leads to better control of the reaction and hence control over the properties of Nanomaterials. There is a strong influence of reactants and stabilizing agents, even prior to nucleation, on the properties of final magnetic nanoparticle obtained through wet-chemical synthesis.
- Appropriate bio-functionalization of both the nanoparticles as well as GMR surfaces needs to be accomplished in order utilizes the magnetic nanoparticles in GMR sensor development.
- While toxicity of the magnetic nanoparticles may not be a major concern as the sensor system is for in vitro assay, it is however, important to understand these effects.
- While results from our investigations reveal a better understanding of the complexity of various issues involved in designing of magnetic nanoparticles, a complete testing of these nanoparticles using the microfluidic GMR platform is essential before the technology is ready for commercialization.

Training & Outreach Activities

The focus was primarily in student training, mainly master and PhD level. They participated in all aspects of the research, especially in the development and fine-tuning of the microfluidic development platform and using it for systematic studies of bio-functionalized sensor surfaces. Some tasks have been addressed by REU students (CAMD has an NSF funded REU program) complementing the DARPA sponsored efforts. Furthermore, in 2005, one of the high school students from Houston, Texas, Ms. Arathi Ramachandran, spent three months in the laboratories of Challa Kumar and participated in the investigation of wet-chemical synthesis of bimetallic nanomaterials.

The results of our efforts have been presented at different conferences and workshops specialized on MEMS and applications in microfluidics. Outreach to the broader public was achieved through invited lectures and especially on CAMD Open House events (typically 400 visitors) once a year. In addition we have a permanent exhibit in the CAMD experimental hall (poster and hardware) show-casing our efforts to approximately 300 visitors every year.

PART 3 – LSUHSC Report
Development of Magnetic Nanomaterials and Devices for Biological Applications
DARPA Grant No. HR0011-04-C-0068

(Subcontractor: LSUHSC)
Louisiana State University Health Sciences Center
Neuroscience Center of Excellence
433 Bolivar Street
New Orleans, LA 70122

Program Director: **Nicolas G. Bazan, M.D., Ph.D.**
Director, LSU Neuroscience Center of Excellence

Project 1: BIO-MAGNETICS INTERFACING CONCEPTS: A MICROFLUIDIC SYSTEM USING MAGNETIC NANOPARTICLES FOR QUANTITATIVE DETECTION OF BIOLOGICAL SPECIES AND AN ANALYSIS OF THEIR POTENTIAL TOXICITY

Mark A. DeCoster, PhD

I. GENERAL PROJECT OBJECTIVE This project has a two-fold purpose: to learn to manipulate and precisely deliver nanoparticles to specific locations within the microenvironment of brain cell cultures, and to determine the potential toxic effect of the presence of these particles on these cultures.

II. TASK OBJECTIVES The main interest of LSU-Neuroscience Center researchers is to study neurochemical mechanisms of brain injury that are of great interest to the military. The final objective of this project is to fill major gaps in our knowledge as to which molecular and cellular mechanisms are critical for the selective brain vulnerability that is impaired in mild traumatic head injury (MTHI) consciousness. We have made use of the magnetic nanoparticle technology that was developed in CAMD and/or AMRI to explore:

1) a more efficient delivery of neuroprotectant drugs
2) signaling mechanisms leading to neuronal cell death
3) ways to prevent undesirable degrading mechanisms due to injuries
4) potential toxic effects caused by the presence of these particles

To these ends we used two main experimental models:

a*) in vivo*: The fluid percussion head injury (FPI) model to reproduce traumatic brain injury (TBI) in the rat so that biochemical, histological and behavioral changes can be followed. Characterization of this TBI model is the first step for the evaluation of neuroprotection by new drugs that will be complexed to nanoparticles for more efficient delivery and faster action.

b) *in vitro*: To develop cellular biomagnetics tools to investigate brain cell signaling and cell injury. Here, there are three objectives: 1) the development of magnetic particles to aid in particle visualization and optimization of cell interaction for cell signaling and drug delivery; 2) the development of a magnetic microscope probe to aid in control of particle cell interaction and drug delivery; 3) to determine the potential toxicity of these particles on theses cell cultures.

III. GENERAL METHODOLOGIES

A. Fluid percussion injury *In vivo* TBI triggers an inflammatory cascade that results in increased blood brain barrier (BBB) permeability, edema and infiltration of leukocytes leading to neuronal cell death. Wistar rats (250-300g body weight) were anesthetized with halothane, and a 4 mm craniotomy was done on the right parietal cortex. A 2 mm female union-bolt was cemented to the skull and animals were left to recover for 24 hours prior to the FPI (3 atm., 100 ms duration). Animals were left for different periods of time, up to 7 days with food and water *ad.lib.* BBB permeability was evaluated at 24, 48 and 72 hrs after FPI by measuring Evans blue dye extravasations.

B. Histopathological analysis Apoptotic cell death was investigated by TUNEL in paraffin sections, using terminal transferase-mediated biotinylated d-UTP nick-end labeling. Immunohistochemical detection of glial fibrillary acidic protein (GFAP), and mieloperoxidase (MPO) was done in deparaffinized and rehydrated sections blocked with 10% normal goat serum for 1h to overnight and GFAP-CY 3 conjugate (1:100) or rabbit anti human MPO (1:100), respectively. The Deconvolution Imaging System was used for analysis and imaging.

C. **In vitro *studies*** Our working model utilizes primary cell cultures of rat brain cells as well as a human umbilical vein endothelial cells (HUVECs). Using these cells in various cell culture dishes and plates allows us to monitor by microscopy magnetic particle-cell interactions both acutely and long-term. We have constructed an electromagnetic probe for our microscopy imaging system, which is positioned in all

3 axes with a manual micromanipulator. In synthesizing fluorescent magnetic nanoparticles, we have used streptavidin- labeled with Alexa 546 to aid in visualization of the particles under the microscope. Acute control of particles is controlled by a variable electromagnetic microscope probe, which we have constructed. Long-term control of particles utilizes a permanent magnet available from Molecular Probes (Invitrogen). We have obtained particles of varying composition, including iron, copper, and cobalt, and have determined the survival rate of hippocampal astrocytes (support brain cells involved in the inflammation process) in cultures that were presented with each type of particle.

IV. TECHNICAL RESULTS

1 **In vivo *studies*: *Traumatic Brain Injury*.** The level of Evans blue recovered from the damage (right) hemisphere was increased 3.9-and 5.0-fold at 24 and 48 h, respectively, while in the contralateral hemisphere these values were 3.3-and 2.4 fold, indicating a lower, although significant, alteration of the BBB and a faster recovery than in the damage site. Histological examination by TUNEL 48 hrs after trauma showed the area of apoptotic cell death and by 7 days reactive gliosis was detected with GFAP in the FPI area. All studies were done in parallel in sham control animals.

2 ***In vitro studies***

1 In collaboration with CAMD, we have synthesized fluorescently-labeled streptavidin-bound paramagnetic particles. We were able to visualize the particles under both phase and fluorescence microscopy, and we could control their position with a magnetic field.

2 We have constructed a useful variable electromagnet that can be positioned with a micromanipulator mounted on a microscope stage to image probe/particle interactions and interactions with cells.

3 We have successfully interacted magnetic nanoparticles with primary cultures of rat neurons and astrocytes. These magnetic particles can be positioned for days at a time with a permanent magnet. After extensive observations of cell cultures, we found that magnetic particles appeared to interact/associate better with astrocytes than with neurons. No cytotoxic effects of long-term particle-cell interaction were observed with these types of particles (produced by CAMD).

4 We have measured the cytotoxic effect of particles of different compositions on cultured endothelial cells and astrocytes. Cobalt has excellent magnetic properties but is slightly toxic. However, when cobalt particles are coated with copper, the level of toxicity increases by 80%. It is, therefore, extremely important to consider the makeup of the nanoparticles that are to be used for drug delivery and in biological reactions.

V. TECHNICAL PROBLEMS ENCOUNTERED AND ATTEMPTED SOLUTIONS

1 We have constructed fluorescent streptavidin-labeled superparamagnetic nanoparticles in collaboration with CAMD. While useful in that these particles retain superparamagnetic properties and some fluorescence, we encountered problems with these particles clumping and aggregating after functionalization (after addition of the fluorescent streptavidin), in comparison with starting particle material. In addition, labeled particles were not uniformly fluorescent, and many were only weakly fluorescent as determined by microscopy.

2 We have constructed a variable electromagnetic microscope probe for controlling particle-cell interactions and drug delivery. In our initial prototype the dissecting pin used to construct the probe, while useful in size and length, retains magnetic properties after removing the electrical current to the probe. More useful would be a probe without a magnetic memory.

3 While we initially utilized fluorescent *macro*particles and successfully localized them in tissues and cultures, it is extremely difficult to localize nanoparticles within cells following internalization. Because they can not be resolved with a light microscope, we used the electron microscope and examined many sections to establish that the particles were, in fact, being internalized. This is a disadvantage of nanoparticle use because of the effort required to visualize and prove that the particles are located within cells.

Project 2: PAIN IN MILITARY PERSONNEL

Anthony L. Vaccarino, PhD and Elena B. Rodríguez de Turco, PhD

I. GENERAL PROJECT OBJECTIVE This project tested specific tailored pharmacological agents for effectiveness in analgesia (pain relief) to find the most efficient compound, and tested the delivery of this compound to a specific damaged tissue with magnetic nanoparticles.

II. TASK OBJECTIVES

The following objectives will be done at LSUHSC-NSC

A To develop candidate analgesic compounds that bear a carboxyl group to be linked to magnetic nanoparticles

B To test the new compounds for analgesia

C To test for liver toxicity.

D To bind the analgesic to nanoparticles at CAMD

E To test *in vitro* the inhibitory effect of the analgesic alone and linked to nanoparticles in the COX-2 enzyme

F To test *in vivo* analgesic effect of analgesic alone and linked to nanoparticles in a model of pain

III. GENERAL METHODOLOGIES

A. Pain assays. *Chemically-induced writhing.* In this model of visceral pain, abdominal contractions (writhing) were induced in mice by an IP injection of 0.4% acetic acid at a dose of 10 ml/Kg. The numbers of writhes, characterized by a wave of contraction of the abdominal muscles followed by extension of the hind limbs, were counted for 10 min beginning 5 min after the acetic acid injection. *Complete Freund's Adjuvant –Induced Thermal Hyperalgesia.* Under halothane anesthesia, mice were injected with 0.1 ml of CFA (Calbiochem, USA) to the glabrous surface of one hind paw. When injected into the foot-pad, CFA produces localized inflammation and hyperalgesia that appears within 2 h and is present for 7 to 10 days. At 48-hours post-CFA (time of peak hyperalgesia) the latency to withdraw the paw from a thermal stimulus was measured using an analgesiometer (IITC Life Sciences, Inc, Woodland Hills, CA). The stimulus intensity will be set to produce baseline latencies of about 10-15 sec, and a 20 sec maximum latency will be used. Thermal hyperalgesia was measured before (pre-drug baseline) and after drug administration.

B. Toxicity assays. Serum transaminase activity (GPT/GOT) After sacrifice, blood was withdrawn into heparinized 1 cc capillary syringes. The blood samples will be spun at 3000 rpm for 10 min in a refrigerated centrifuge to separate plasma. The GPT and GOT levels were determined spectrophotometrically using Sigma kits. *Glutathione depletion.* After sacrifice, the livers will be perfused with heparinized saline. The right half of the main lobe was removed and homogenized using Teflon pestle in MPA (5% w/v) to a concentration of 5% (w/v). The homogenate was centrifuged at 3000 G for 10 min at 4°C, and glutathione levels were measured in duplicate on 300: 1 aliquots of the supernatant using a standard colorimetric assay.

C. COX-2 assay in HUVEC's cells HUVECs were obtained from BioWhittaker (Cambrex). Cells were used in passage 3-7. Cells were grown in EGM2 (BioWhittaker, Cambrex) to75-85% confluence in a 370C incubator/CO2 5% and then plated in 6-wells plates. For COX-2 induction, the cells were starved overnight in EBM + 2% FBS followed by 24 h incubation in EGM2 media containing 2% FBS prior to the addition of IL1 alpha (4 µl, 2µl/ml in 0.9% saline containing 1%BSA). The media from HUVECs cultures activated with IL1 alpha was changed to Hank's solution, 0.75% BSA. SCP-22 suspended in DMSO/media and SCP-22 bound to NP suspended in media was added to the wells (20 µl; final conc. DMSO in the wells 0.01%). Controls received the same volume of the vehicle (DMSO or NP). After 30 min incubation at 370C in a shaking incubator, AA was added (final conc 2 µM) and the cells further incubated for 15 min. The media was collected for prostaglandin E2 (PGE2 analysis by EIA (Cayman)) following kit instructions.

IV. TECHNICAL RESULTS

1 Analgesia Of the 3 synthesized compounds that beared the requisite carboxyl group, one compound SCP-22 showed good analgesic activity. A 3 mmol/kg oral dose of SCP-22 showed analgesic activity that was confirmed in 2 pain assays (Complete Freund's Adjuvant-induced hyperalgesia and chemically- induced writhing. Because low amounts of SCP-22 are generated through chemical synthesis (see Technical Problems) the analgesic effects were also determined for SCP-22 when administered

intrathecally (at 15 minutes post injection). It was found that when administered intrathecally SCP-22 retained its analgesic effect.

2 Toxicity A 6 mmol/kg oral dose of compound #22 did not produce hepatotoxic effects (it did not deplete liver glutathione and did not elevate plasma transaminase activity).

3 Binding of Analgesic to Magnetic Nanoparticles Because SCP-22 has a carboxyl group in C2 and showed good analgesic activity and low toxicity, the possibility of binding this drug to magnetic nanoparticles was explored. SCP-22 was sent to CAMD and Dr. Challa Cumar linked the drug to magnetic nanoparticles (MNP) using carbodiimide chemistry. The drug-NP complex sent from CAMD to LSUHSC contained 3.7 mg of SCP-22 bound to 24 mg drug-NP. Analysis by HPLC at CAMD indicated that the drug was successfully bound to MNP.

4 In vitro activity of SCP-22-MNP (Inhibition of COX-2 enzyme) The biological activity of the bound drug as inhibitor of COX-2 was tested in HUVEC's cells. SCP-22-NP did inhibit COX-2 although with less efficiency than SCP-22 in DMSO. Although a shaker incubator was used, there was not a good homogeneous distribution of the drug-NP above the cells. This could explain the lower inhibitory effect as compared to drug/DMSO.

***5 In vivo activity of SCP-22-MNP (Analgesia)*:** The biological activity of SCP-1 bound to nanoparticles was determined after intrathecal administration in the CFA assay. It was found that SCP-22 retained its analgesic effects when bound to MNP.

V. TECHNICAL PROBLEMS ENCOUNTERED AND ATTEMPTED SOLUTIONS

To date, one compound (SCP-22) derived from SCP-1 has been prepared and tested for analgesic activity, liver toxicity and its inhibitory action on COX-2 enzyme. Because low amounts are generated through chemical synthesis and subsequent binding to NP, no studies given the drug ip or iv can be performed. Therefore, to allow us to study the effects of the drug in small quantities in vivo the NP bound compounds were administered intrathecally (ie., spinal).

Project 3: PROTECTING RETINAS FROM LASER-INDUCED INJURY: THE DEVELOPMENT OF A TISSUE-SPECIFIC DRUG DELIVERY SYSTEM

William C. Gordon, PhD

I. GENERAL PROJECT OBJECTIVE Development of a drug delivery system designed to deliver small volumes of highly concentrated pharmacologic compounds to specific tissues utilizing biomagnetic nanopartical technology.

II. TASK OBJECTIVES

1 To develop a light-induced retinal damage model.
2 To define the effect of bright light
3 To demonstrate retinal neuroprotection in the bright light model.
4 To demonstrate that super-paramagnetic particles can be localized within the retina by a strong magnetic field
A. Localization of [^{3}H]leucine-labeled super-paramagnetic nanoparticles and directed delivery to retinal tissue by a magnetic field.
5 To define the effect of laser damage on retinal tissue
6 To stimulate new blood vessel growth in retina with small laser burns
7 To "associate" a neuroprotective compound with super-paramagnetic nanoparticles
8 To systemically deliver neuroprotectant-labeled super-paramagnetic nanoparticles to retina
9 To concentrate and retain these particles *in situ* with a strong magnetic field
10 To demonstrate release of the neuroprotectant from the nanoparticles and show a subsequent reduction of the laser-damaged retinal area

III. GENERAL METHODOLOGIES

A. Animals The Louisiana State University Health Sciences Center Institutional Animal Care and Use Committee reviewed and approved these experimental procedures which are in accordance with both the Association for Research in Vision and Ophthalmology Statement for the Use of Animals in Ophthalmic

and Vision Research and the Guiding Principles in the Care and Use of Animals of the National Institutes of Health (Publication 86-23). Sprague-Dawley male rats (150-175 g) and C57BL/6 mice, obtained from Charles River, were fed rat or mouse chow and given water *ad libitum*. They were acclimated for at least 5 days (12 hours dark: 12 hours dim overhead fluorescent light; 7.1 Lux average front to back within covered, tinted, forced-air cages; light onset 0600 hours) prior to experiments.

B. Light damage model To study retinal damage and test neuroprotective compounds, we have constructed a fluorescent light stimulator consisting of an array of eight circular fluorescent light bulbs, 10 inches in diameter, which supplies 18,000 lux. A divided Lucite tube, accommodating 2 rats (eyes dilated), was inserted into the center of the array for varying lengths of time. We have found that the optimum duration of light treatment is 5 hours.

C. General tissue preparation Eyes were collected, corneas slit, and whole eyes placed in fixative overnight at 4 °C. Whole eyes were then cut in half through the optic nerve along the superior-inferior meridian, and the superior cornea notched for orientation from light microscope sections. Eye cups were then returned to fixative for at least 1 additional hour.

D. Light and electron microscopy Eyes were placed in fixative overnight at 4 °C: 10% neutral buffered formalin (EM Science, Gibbstown, NJ) for 20 µm-thick cryo-sections; 2% glutaraldehyde and 2% paraformaldehyde in 0.135 M sodium cacodylate for plastic light and electron microscopic sections. Whole eyes were cut in half through the optic nerve along the superior-inferior meridian, and the superior cornea notched for orientation from light microscope sections. After an additional hour in primary fixative, hemisected eyes for frozen sections were cryoprotected in PBS containing 30% sucrose overnight at 4 °C. Frozen sections were used for immunolocalization. Eyes for plastic embedding were rinsed in sodium cacodylate buffer, post-fixed in osmium tetroxide (1% for 1 hour) in buffer, and rinsed again. Tissues were dehydrated through a 20% stepped ethanol series to acetone, infiltrated, and embedded in an Embed-812/Araldite 506 mixture (Electron Microscopy Sciences, Fort Washington, PA). Thick plastic sections (1 µm) were stained with toluidine blue and viewed with bright-field microscopy. These sections were used to construct the retinal profiles for each light treatment paradigm. The superior-central portion of each retina was identified by the corneal notch and the corresponding block trimmed to remove the peripheral and inferior retina. These smaller, oriented blocks were then sectioned for electron microscopy. Silver-gold sections were collected on nickel grids, stained for contrast with lead and uranium salts, then viewed and photographed with a JEOL 1210 or a Zeiss 110c transmission electron microscope.

E. Immunohistochemistry Immunolocalization of antibodies was performed on cryo-sections (20 µm thickness). Briefly, sections on glass slides were fixed in cold methanol, followed by antigen retrieval and blocking for 1 hour. Sections were treated with primary antibodies for up to 42 hr, rinsed, and fluorescent secondary antibodies added for 2 hr. Slides were rinsed, coverslipped, and examined by deconvolution or confocal microscopy (Zeiss systems with appropriate software).

F. Western blotting Retinas were homogenized at 4° C in PBS, pH 7.2, with broad-spectrum protease inhibitors (78410 Halt Cocktail; Pierce, Rockford, IL) and proteins quantified by Bradford microassay. 15 µg were loaded onto each lane on Tris-HCl Criterion Precast Gels (Bio-Rad #345-0028) and then blotted onto PVDF membranes. Blots were probed with appropriate primary antibodies (Santa Cruz Biotechnologies). Bound primary antibodies were detected by anti-"animal" IgG fluorescein-linked secondary antibodies, and were developed with a Western Blot Analysis System according to manufacturer's instructions (RPN5780 ECF Western Blotting Kit; Amersham, Arlington Heights, IL). Detected bands were digitized and density profiles constructed for final analysis.

G. Retinal neuroprotection LAU-0901, a platelet activating factor receptor blocker, is neuroprotective in brain. Following one intraperitoneal injection (30 mg/kg body weight in 45% cyclodextrin in saline) two hours prior to light stimulation, rats were exposed to five hours of light and returned to darkness until retinas were analyzed.

H. Laser-induced retinal damage Following anesthetization, mice were dilated and placed in a holder on a slitlamp. A drop of methyl cellulose was placed on the eye and a small square of plastic situated on top to subtract the optical effects of the cornea and lens. The optic nerve was localized with the slitlamp

and 6 laser burns were made at 500 um from the optic nerve at 1, 3, 5, 7, 9, and 11 o'clock. Each 50 um-diameter burn was made at 100 mW of power for 0.2 seconds. A successful burn made a flash, followed by a white hole through the back of the retina. Mice were allowed to recover from anesthesia and then returned to the animal colony until retinas were collected.

***I. Directed delivery and localization of nanoparticles* in vivo** Labeled (fluorescence of tritium) super-paramagnetic micro- or nanoparticles were resuspended in 0.5 ml saline, sonicated for five min, and 50 µl injected into the femoral vein of anesthetized adult male mice. These mice were then placed on the surface of a 4.5 kG magnet (Molecular Probes) for up to one hour with one eye contacting the surface, or one ear taped flat to the magnet. Mice were killed and tissue rapidly collected. The "magnet" ears and eyes were compared to the "nonmagnet" ears and eyes. Tissues were solubleized and aliquots analyzed by scintillation counter for levels of tritium (nanoparticles) or by fluorescence microscopy of cryosections.

J. [^{3}H]leucine binding to super-paramagnetic nanoparticles Ten-nm-diameter super-paramagnetic nanoparticles were fabricated for us by CAMD and amino groups attached to the surfaces. Under the guidance of CAMD, we attached [^{3}H]leucine to these groups to make it possible to localize the particles within tissues by scintillation counting. Five mg of nanoparticles were dispersed in 0.5 ml distilled water and sonicated under nitrogen for two min. Carbodiimide (4.2 mg; Sigma), dissolved in 0.15 ml water was added and the mixture sonicated for two min. After cooling on ice, [^{3}H]leucine (2.5 to 50 µCi in 125 µl water; SA = 125 Ci/mmol) was added and the sample incubated for two hours at 4^0 C. The nanoparticles were retained on the sides of the reaction tube with a magnetic field and washed with 0.5 ml water five times until minimal radioactivity was detected. Under these conditions, 10% of the [^{3}H]leucine was bound to the nanoparticles. Additional washes continued to extract label until background was finally reached, indicating weak or non-ionic bonding to particles.

K. "Association" of neuroprotectant, LAU-0901, with 15 nm super-paramagnetic nanoparticles In another set of experiments (See *III. General Methodologies; J*), it was noted that molecules (e.g., amino acids) are not always linked to the nanoparticles, but become weakly associated. These molecules are slowly released during subsequent washes. It has been a concern that if specific molecules were linked to nanoparticles for delivery to specific tissues, they could not be released at the damage site because of the chemical linkage. We, therefore, designed two experiments to only "associate" the neuroprotectant LAU-0901 with the super-paramagnetic nanoparticles. LAU-0901 was sent to LSU-CAMD where Dr. Kumar and his associates conducted two incubations; LAU was mixed with cyclodextran-β, the normal solvent used for animal tissue delivery. 15 nm super-paramagnetic nanoparticles form CAMD were incubated in this mixture, washed, dried, and returned to the LSU-Neuroscience Center. In the second incubation, LAU was added to methanol and then incubated with the nanoparticles. After drying, these were also returned to LSU-NC. Both mixtures were injected into the femoral veins of anesthetized mice, and the right eyes placed on a strong magnet for 30 minutes. To be sure particles were being circulated systemically, some mice were not placed on magnets. Right "magnetic" and left "control" eyes, and both eyes from the non-magnet animals, were then removed and the retinas prepared for analysis by mass-spectrometry by placing in 500 µl of methanol.

IV. TECHNICAL RESULTS

1 To develop a light-induced retinal damage model We have shown that when rats are placed in a plastic tube within the light stimulator for five hours, photoreceptor death is initiated. Within three days, photoreceptors have undergone apoptosis and have been removed. Five hours was selected because approximately 50% of these cells were lost. This makes the results of drug testing more meaningful because the effect can be measured as either plus or minus. Histological examination of these retinas indicated that this damaging stimulus was specific for photoreceptors, and damage was centered around the superior central portion of the retina, the "sensitive spot" in rodents. Structural analysis of retinal tissues demonstrated that photoreceptor organelles and membranes remained intact, while nuclei began to darken, disorganize, and bleb. These are hallmarks of apoptotic cell death (programmed cell death requiring the up-regulation of specific genes to trigger enzymatic degradation of the nucleus, as opposed to necrosis). This model was used to establish the events leading to neuronal apoptotic cell death and to

provide a system upon which to test neuroprotectants. Finally, this information was applied to retinas that had been laser damaged.

2 To define the effect of bright light on photoreceptors Using the light damage rat model, we have established a *sequence of events* that occurs as oxidative stress is triggered within neurons (photoreceptors):

A Mitochondrial protein import systems are altered.

B Mitochondria begin to undergo division and migrate toward the nucleus.

C Guanine within mitochondrial DNA becomes oxidized, and is converted to the mutagen 8-oxoguanine.

D The repair enzyme 8-oxoguanine-DNA-glycosylase is up-regulated to convert 8- oxoguanine back to guanine.

E Mitochondrial DNA begins to undergo fragmentation

F The mitochondrial DNA repair enzyme DNA polymerase γ is up-regulated.

G *If mDNA is adequately repaired, photoreceptors will survive* the insult and mitochondria will undergo fusion; if not:

H Cell death-signaling molecules from mitochondria are released into the cytoplasm and activated.

I Nuclear DNA begins to undergo fragmentation.

J The nuclear DNA repair enzyme DNA polymerase β is up-regulated.

K *If nDNA is adequately repaired, photoreceptors will survive* the insult; if not:

L Apoptotic cell death occurs.

Mitochondrial pellets from retina were incubated with an antibody against the mitochondrial outer membrane translocase TOM-20, rinsed, and then incubated with 10 nm diameter immunogold particles to demonstrate:

a. an antibody against the molecule of interest could be used to tag a pure preparation of mitochondria for easy sample scoring of "present" or "not present" at electron microscope level;

b. the feasibility of using an organelle-specific antibody in conjunction with 10 nm immuno*magnetic* particles to aid in panning and isolation of photoreceptor organelles exhibiting alterations following damaging light.

The technique was successful; gold nanoparticles were observed to decorate mitochondrial membranes in sections from pellets that were plastic embedded. It may be possible to specifically target damaged organelles.

3 To demonstrate retinal neuroprotection in the bright light model We have shown that pretreatment with the LAU-0901 compound protects photoreceptor cells from light-induced apoptotic death. Pretreatment with LAU-0901 by i.p. injection 2 hours prior to the 5 hours of light treatment offers 50-75% photoreceptor neuroprotection. These retinas were compared to control vehicle-injected retinas plus 5 hours of light, and showed the usual 50% photoreceptor cell loss 10 days after treatment.

4 To demonstrate that super-paramagnetic particles can be localized within the retina by a strong magnetic field *Proof of principle – localization of nanoparticles in mouse ears placed on a magnet.* One um-diameter fluorescence-labeled (FITC) super-paramagnetic macroparticles (Polysciences) were injected into the femoral veins of anesthetized mice; the right ear of each was taped to a strong magnet (Polysciences, 4.5 kG) for 30 minutes. Animals were killed *in situ* by over-injection of ketamine, and the ears removed and dropped into liquid nitrogen. (n.b., The ears that were taped to the magnet were attracted to the magnet after being removed, suggesting they contained a high concentration of metallic particles.) Following tissue preparation for cryo-sectioning, unstained sections were examined by fluorescence microscopy for evidence of fluorescent particles. Particles were present, but, because only cross sections of capillaries could be observed, the number of particles was very small. It is important to know the tissue uptake rate of the particles, percent delivery of total particles, and the percent retention. However, analysis of tissue sections for fluorescent particles is not adequate. Therefore, we attempted to quantify the delivery of particles to the retina throughout a time course using radioactive tracers.

Working with CAMD, we attached ^{3}H-labeled leucine to their 10 nm super-paramagnetic nanoparticles, which are below the resolving power of the light microscope. Solutions were treated with a strong magnetic field to isolate the particles, followed by repeated decanting and washing. Release of the field allowed the particles to be resuspended. Following each wash, an aliquot of the wash liquid was counted by scintillation counter. This demonstrated that for each wash, radioactivity was released. This activity may have been from individual labeled particles that could not be held by a magnetic field. However, each wash continued to show radioactive label, suggesting that the amino acid was either not well attached to the particles, or that it was merely "associated" with them. Attempts to quantify radio-labeled particle uptake in tissues were abandoned.

Fluorescent super-paramagnetic microparticles (1-2 μm) were injected into the femoral vein of anesthetized mice while the right eye was resting on a strong magnet. Animals were killed in situ by overdose of ketamine, and eyes collected and prepared for cryo-sectioning. We observed that a strong magnetic field appears to concentrate particles within the retina. Using *retinal flat mounts*, rows of fluorescent beads were observed within the capillary beds, demonstrating that the retinal vasculature could be targeted systemically. In several instances, fluorescence was observed in the choriocapillaris just behind the retinal pigment epithelium. However, because of retinal thickness and the three layers of retinal blood vessels, it is difficult to quantify the label. It is from capillaries within this location behind the eye that photoreceptors exchange molecules, and it is from here that neuroprotective drugs would enter the retina. *Using a strong magnetic field on the eye, it is possible to concentrate magnetic particles within the capillaries of the retina.*

5 To define the effect of laser damage on retinal tissue To demonstrate consistent delivery of retinal laser burns and to observe the efficacy of LAU-0901 (a neuroprotective PAF receptor blocker), we employed a Novus Omni argon photocoagulator laser from the LSU Department of Ophthalmology to perform initial laser retinal ablations in mice. These mice were pretreated with LAU-0901 or vehicle-alone, two hours prior to laser treatment. 800 mW of energy was applied to four 500 μm diameter regions per retina for 200 mS duration to insure that Bruch's membrane had been ruptured. Burns were examined in retinal eyecup whole-mount preparations prior to histological examination. Preliminary observations suggest that by 6 days post-treatment, damaged regions had expanded in the vehicle-alone treatments, fusing in some cases, while LAU-treated retinas appeared to have well defined edges to the burn spots (i.e., no fusion from lateral spreading). Microscope sections through burns showed neovascularizing plugs forming after 6 days. However, when LAU- and vehicle-alone treatments were compared, the LAU-0901-treated retinas appeared to have a thinner region of neovascularization. The control burns had more red blood cells than the LAU burns, suggesting that LAU-0901 exerts a regulatory effect on laser-induced choroidal-neovascularization.

Our *Spectra Integrated Laser System* (Novus Spectra Diode-pump) allowed us to deliver variable sized burns at variable energies to mouse retinas through slit lamp optics. Histological examination of laser-damaged retinas throughout a time course, consisting of 0, 2, 4, 6, 12, 18, and 24 hours after burns, and 2, 4, 6, 8, 10, 14, and 20 days after burns, revealed:

1. Bruch's membrane, separating retina from the underlying capillary bed (choriocapillaris), is perforated at an energy of 100 mW for 200 mS at a beam diameter of 50 μm.
2. Photoreceptors and the retinal pigment epithelial cells die at the site of the laser burn.
3. The retina in the area adjacent to the burn detaches, probably from the formation of steam.
4. Endothelial cells from behind the retina are triggered to divide.
5. These nascent blood vessels invade the photoreceptor layer of the retina, ramify, and grow.
6. This neovascularization causes retinal detachment, triggers damage lateral to the initial wound, and spreads.
7. (Incidentally) This is an exact description of what occurs in age-related macular degeneration (ARMD), so defining the process of retinal degeneration triggered by laser damage also defines the process of vision loss by ARMD.

The retinal laser burns produce a response in the mouse retina that very closely mimics that observed in human retinas with Age-related Macular Degeneration; pretreatment with LAU-0901 appears to slow or inhibit the lateral spread of laser-induced damage.

6 To stimulate new blood vessel growth in retina with small laser burns Immunohistochemical localizations were made of the first set of laser burn samples at ten days following the burns. Molecules associated with choroidal neovascularization were identified within the laser burn regions of the experimental retinas, but not in control retinas. Specifically, *β-amyloid pre-protein* (the same molecule associated with Alzheimer's disease) and *vascular endothelial growth factor (VEGF*) were localized, indicating that the process of chorio-neovascular-ization had been triggered by the laser burns. β-amyloid pre-protein has been found in damaged retina and can be used as an indicator for damage. VEGF is up-regulated in tissues when new capillary growth is initiated. An extended time course was conducted in which mice were maintained at various times following laser treatment to the *right* retina only. These times were 0, 2, 4, 6, 12, 18, and 24 hours after burns, and 2, 4, 6, 8, 10, 14, and 20 days after burns. Six animals were treated at each time point; the *left* untreated retinas served as controls. Each animal received 6 burns arrayed radially around the optic nerve at 1, 3, 5, 7, 9, and 11 o'clock. Retinas were collected and examined histologically for laser damage. This examination entailed a description of cells from the choriocapillaris (from behind the retina), which invade the retina through the burn hole, mimicking the human retinal response to laser damage. These cells are the pigment epithelial cells and newly formed blood vessels from behind the retina.

Three antibodies were localized within the damaged regions of these retinas: Cyclo-oxygenase-2 (COX-2), an indicator of inflammation; Tissue necrosis factor alpha (TNFα), an indicator of inflammation and an inductor of macrophages; Vascular endothelial cell growth factor (VEGF), an inducer of new blood vessel growth. COX-2 appeared by 18 hours, lasting to about 10 days; TNFα occurred from day 6 through day 14; VEGF was found from day 6 through day 20. This indicated that following the initial inflammatory response, macrophages were summoned to clean up the burn site, shortly followed by the induction of new blood vessel growth within the damaged region of the retina.

The laser-induced retinal damage activates an inflammatory response and signaling from the damage site for white blood cell (macrophage) influx. These events are followed by initiation of neovascularization and vessel growth into the damaged region.

7 To "associate" a neuroprotective compound with super-paramagnetic nanoparticles Dr. Kumar and his associates at LSU-CAMD weakly associated LAU with their 15 nm super-paramagnetic nanoparticles. Samples of these particles were analyzed by mass-spectrometry (Dr. Marcheselli, LSU-NC) to determine if LAU was present. Particles with LAU in cyclodextrin-β appeared to retain about 10%; particles with LAU in methanol retained about 25%. *Compounds such as the neuroprotectant LAU-0901 can be weakly "associated" with super-paramagnetic nanoparticles, suggesting that quick, systemic delivery to damaged nervous tissue, followed by concentration and retention there with a magnetic field, may be sufficient to release adequate protectant.*

8 To systemically deliver neuroprotectant-labeled super-paramagnetic nanoparticles to retina The two solutions of LAU-associated nanoparticles (LAU-cyclodextran-β and LAU-methanol), prepared by LSU-CAMD (Dr. Kumar and his associates), were injected systemically into anesthetized mice. After 30 min, the right and left retinas from these animals were collected and prepared for mass-spectrometry. These samples have not yet been analyzed.

9 To concentrate and retain these particles* in situ *with a strong magnetic field Both mixtures were injected into the femoral veins of anesthetized mice, and the right eyes of these animals placed on a strong magnet for 30 min. Right "magnetic" and left "control" eyes were then removed and the retinas prepared for analysis by mass-spectrometry. These samples have not yet been analyzed.

10 To demonstrate release of the neuroprotectant from the nanoparticles and the subsequent reduction of the laser-damaged retinal area Preliminary results from the early laser burn experiments suggest less retina damage in laser-treated mouse retinas pre-treated with LAU-0901. The region immediately surrounding the laser burn becomes damaged and gradually enlarges to its final diameter in about 2 weeks. The first experiments with LAU suggested that this final diameter was reduced, i.e.,

retinal neurons were protected. Laser-damaged retinas from mice treated and not treated with LAU-associated nanoparticles were collected and are being examined for damage.

V. TECHNICAL PROBLEMS ENCOUNTERED AND ATTEMPTED SOLUTIONS

1. Developing an appropriate magnetic field for the retina We attempted to fabricate an electromagnet by wrapping lacquered copper wire around an iron rod and connecting this to a variable power supply. The end of the iron rod was machined so that it would fit onto the cornea of the mouse eye much like a contact lens, allowing the full force of one pole of this bar magnet to impinge on the eye. It was hoped that this would maximally concentrate the nanoparticles within the capillaries of the retina. However, when activated, the iron bar got so hot that it could not be touched. Further trials with fewer coils on the iron bar and the addition of a steel pin produced a very small point source that we could use to manipulate small quantities of particles. We purchased a flat, very strong (4.5 kG) permanent magnet from Molecular Probes. This has subsequently been used during this project.

2. To verify the presence of, and to quantify, nanoparticles within specific tissues It is a problem to quantify and verify the existence of nanoparticles within tissue. We began with 1-μm-diameter fluorescent microparticles (Polyscience). When placed in a magnetic field, these particles aligned, and could be viewed with fluorescence microscopy. When injected into the femoral vein of mice, fluorescent particles could be observed lined up within the capillaries of the retina, indicating that they could be dispersed throughout the circulatory system. However, smaller particles (< 100 nm) are not visible by light microscopy, and very small objects have decreased surface area (lower fluorescence). We, therefore, assumed that invisible nanoparticles would behave as did the visible microparticles. However, showing *direct* evidence that nanoparticles are present within a specific tissue remains a problem. We attempted to address this by labeling nanoparticles with tritiated leucine. We reasoned that once tissue delivery was accomplished, we could homogenize the tissue and quantify the radiation by scintillation counting. However, we learned that the label continued to come off in successive washes. We still have no direct method of verification or quantification. We are now examining retinas to determine the extent of the laser damage. At this point, we must assume that the nanoparticles are present if we detect a reduction in damage diameter at the laser burn site.

3. To develop a method that will bind a neuroprotectant during transport, but then release it at the damage site There are several means of attaching molecules to metallic nanoparticles, but these require the formation of a covalent linkage, making it questionable whether these molecules can be detached within damaged tissue. We have taken another approach. We have attempted to weakly associate the neuroprotectant with the super-paramagnetic nanoparticles. This appears to be working. LAU comes off the nanoparticles, but slowly. We feel that by injecting LAU-associated nanoparticles in PBS and quickly placing the eye on a magnet, the particles will be rapidly sequestered within the mouse retina. Some LAU will be lost, but much will be gradually released into the retina as the particles are being held in place by the magnetic field. This is being analyzed by mass-spectrometry. This is a promising approach that does not require sophisticated, and perhaps dangerous chemical manipulation at the damage site.

MAJOR ACCOMPLISHMENTS The findings of each of these DARPA projects provided insight into potential methods of neuroprotection and pain alleviation, which could lead to new therapies for military personnel as well as for civilians in the clinical arena.

Project 1: FPI is an excellent model that we plan to use in the near future to test the therapeutic effect of new drugs delivered attached to biomagnetic nanoparticles. *In vitro* studies with brain cells in culture have allowed us to develop a fluorescent streptavidin- labeled magnetic particle that associates with cells, and we have also developed a magnetic microscope probe that allows us to better control position and association of the particles in relation to the cells of interest. These developments may aid in delivery of potentially neuroprotective drugs in the short term *in vitro*, and ultimately, *in vivo*. In collaboration with CAMD we have successfully constructed fluorescent, streptavidin-labeled superparamagnetic nanoparticles that adhere to astrocytes from the brain. This adherence has allowed us to investigate particle-cell interaction with the aid of a magnetic microscope probe which we have constructed.

Attachment of these magnetic particles to living cells may be used to investigate in the future, stress initiated signal transduction such as calcium influx. We have demonstrated in two cell culture models, effects of long-term interaction of cells with magnetic nanoparticles. In brain cell cultures, particles interact mainly with astrocytes, and we have also demonstrated cell interaction with particles using HUVECS. These long-term studies will be important for investigating possible long-term side effects of particles in association with cells, which needs to be determined for further development of particle-based drug delivery. While primary brain cell cultures will serve as an excellent model for investigating cell signaling and injury in the brain, the HUVECs culture model will be a more straightforward system for investigating development and delivery of anti-inflammatory drugs of potential therapeutic interest. We have also shown that nanoparticles containing exposed cobalt are toxic to endothelial cells and nerve cells in culture. Additionally, copper particles are very toxic, and copper-coated cobalt particles exhibit the greatest toxicity. However, cobalt particles have excellent magnetic properties, making them very useful in magnetically manipulated tissue delivery of pharmacological compounds. Cell toxicity can be greatly decreased by coating these particles with other shielding molecules; gold coating eliminates cell toxicity to cobalt. This is especially important because there are long-term deleterious side effects in the brain from the presence of metals, with both aluminum and iron being implicated in Alzehiemer's dementia, and iron implicated in Parkinson's disease. The toxic properties of nanoparticles *must* be considered when applying this technology to areas within medicine.

Project 2: SCP-22 proved to be an excellent analgesic that alleviated pain without the hepatotoxic (liver side effects) characteristic of acetaminophen. The results obtained with this drug bound to nanoparticles indicates that the drug retains its biological activity both *in vitro* and *in vivo,* and suggests that SCP-22 is a good candidate to further explore this new approach of drug delivery in pain assays. However, there was some indication that SCP-22 was rapidly released from the nanoparticles, suggesting that it will be important to carefully consider the release window and delivery time when applying this methodology to medical technology.

Project 3: We have a functioning light damage model with which we have demonstrated that we have a photoreceptor neuroprotective compound that can be used in later phases of this study. We have not yet conclusively demonstrated that drug-labeled super paramagnetic particles can be directed systemically to localize within specified tissues with a magnetic field in this study, but final histological analysis of the experimental retinal treatments should provide this information. This is an important study for two reasons. First, it is an attempt to establish a method to deliver very small (and therefore, less damaging) quantities of drugs only to the precise location where they are needed. Second, the use of retinal laser burns as a damage model is very appropriate because the barrier behind the retina is breached, allowing capillaries to invade the retina in the area where the photoreceptors are located. This triggers photoreceptor death in a manner exactly like that in age-related macular degeneration. Therefore, if we can deliver a neuroprotectant to the retina, *and* reduce the amount of photoreceptor cell loss surrounding the laser burn site, this study will have contributed significantly to understanding and prevention of this blinding eye disease.

TRAINING AND OUTREACH The present DARPA grant has contributed to consolidate several programs that extend training opportunities to students and researchers at various stages of their careers. One of the impacts of this grant has been on the Interdisciplinary Graduate Program in the Neurosciences and on the Summer Undergraduate Program in the Neurosciences, both run by the LSU Neuroscience Center. These programs bring graduate and undergraduate students into a nurturing mentorship environment, one that this grant has helped to foster. The investigators of the projects funded by this grant, in turn, are able to provide valuable insight to the undergrad, graduate students, and research assistants who work and study under them.

Research programs on the molecular and cellular bases of neurological diseases are the heart of the Center's innovative educational programs. The Interdisciplinary Neuroscience Graduate Program (M.S. in Neuroscience, Ph.D. in Neuroscience) attracts outstanding students from around the world; the Summer Undergraduate Neuroscience Program mentors top Louisiana undergraduate students through

lectures and hands-on research; and postdoctoral fellowships train the next generation of investigators. The center also collaborates with other universities to provide training for students pursuing a career in the sciences. For example, in terms of minority outreach we mentored several students from Xavier University of Louisiana during the summer of 2007.

The projects conducted under this grant have played an integral role in allowing students and other researchers to participate in experiments, helping them to build upon their experiences working in a laboratory environment and to expand their knowledge within the realm of the neurosciences.

REPORT DOCUMENTATION PAGE

Form Approved
OMB No. 0704-0188

PLEASE DO NOT RETURN YOUR FORM TO THE ABOVE ADDRESS.

1. REPORT DATE *(DD-MM-YYYY)*	2. REPORT TYPE	3. DATES COVERED *(From - To)*
10-30-2007	FINAL TECHNICAL REPORT	15 Aug 2004 - 14 May 2007

4. TITLE AND SUBTITLE

Development of Magnetic Nanomaterials and Devices for Biological Applications

5a. CONTRACT NUMBER

HR0011-04-C-0068

5b. GRANT NUMBER

5c. PROGRAM ELEMENT NUMBER

6. AUTHOR(S)

O'Connor, Charles J.; Hormes, Josef; and Bazan, Nicolas G.

5d. PROJECT NUMBER

5e. TASK NUMBER

5f. WORK UNIT NUMBER

7. PERFORMING ORGANIZATION NAME(S) AND ADDRESS(ES)

University of New Orleans
Advanced Materials Research Institute
2000 Lakeshore Drive
New Orleans, LA 70148

8. PERFORMING ORGANIZATION REPORT NUMBER

9. SPONSORING/MONITORING AGENCY NAME(S) AND ADDRESS(ES)

DARPA/CMO
Attn: Michael Mutty
3701 Fairfax Drive
Arlington, VA 22203-1714

10. SPONSOR/MONITOR'S ACRONYM(S)

11. SPONSOR/MONITOR'S REPORT NUMBER(S)

12. DISTRIBUTION/AVAILABILITY STATEMENT

Approved for public release; distribution unlimited.

13. SUPPLEMENTARY NOTES

The views and conclusions contained in this document are those of the authors and should not be interpreted as representing the official policies, either expressly or implied, of the Defense Advanced Research Projects Agency or the U.S. Government.

14. ABSTRACT

This report describes a research project in the area of bio-magnetic interfacing concepts aimed at the development of magnetic nanomaterials and devices for biological applications. Novel bio-compatible ferrofluids of functionalized magnetic nanoparticles suitable for bioconjugation of antibodies or other active biomolecules are developed, prepared, and tested for use in biomedical research, and various biological and clinical diagnostic applications.

15. SUBJECT TERMS

biomagnetic interfacing concepts, functionalized magnetic nanoparticles, detection of biological species, biocompatible ferrofluids

16. SECURITY CLASSIFICATION OF:			17. LIMITATION OF ABSTRACT	18. NUMBER OF PAGES	19a. NAME OF RESPONSIBLE PERSON
a. REPORT	b. ABSTRACT	c. THIS PAGE			Charles J. O'Connor
U	U	U	UU	40	19b. TELEPHONE NUMBER *(Include area code)* (504) 280-6840

Reset